Quantum diffusion of positive muons in copper

R. Kadono,* J. Imazato,† T. Matsuzaki,‡ K. Nishiyama,
K. Nagamine, and T. Yamazaki§
Meson Science Laboratory, Faculty of Science, University of Tokyo, 7-3-1 Hongo, Bunkyo-ku Tokyo 113, Japan

D. Richter** and J.-M. Welter
Institut für Festkörperforschung, Kernforschungsanlage, Jülich GmbH, Jülich, Federal Republic of Germany
(Received 25 January 1988; revised manuscript received 6 July 1988)

The diffusion of positive muons ($\mu^+ \approx 0.11 \times$ proton mass) in copper was studied experimentally by the zero-field muon-spin-relaxation method in a temperature (T) range from 70 mK to 190 K, using a pulsed muon beam suitable for the present method. The measurements were performed in three copper samples of different purities to see the effect of impurities on the nature of the μ^+ diffusion. We find that the diffusion (hopping) rate ν in ultrapure copper decreases rapidly with decreasing temperature, reaches a minimum at $T = 30$–70 K, then begins to *increase*. The T dependence in the low-temperature region follows $T^{-\alpha}(\alpha \simeq 0.67 \pm 0.03)$ at 0.5–10 K and levels off below 0.5 K. The behavior is strongly modified by impurity consisting of ≈ 100 ppm iron below 10 K. The T dependence in the pure copper is accounted for by new theories developed independently by Kondo and by Yamada, predicting a hopping rate $\nu \propto T^{2K-1}(0 \le K \le \frac{1}{2}$ for a single charged particle), where the factor T^{2K} comes from the renormalization of the muon tunneling matrix due to the nonadiabaticity of the conduction electron interacting with the moving muon. From the present results the constant K is determined to be $K = 0.16 \pm 0.01$.

I. INTRODUCTION

The positive muon (μ^+) is a radioactive probe produced by high-energy particle accelerators. It has spin $\frac{1}{2}$ and mass 105.7 MeV/c^2, decays into a high-energy positron and two neutrinos with a lifetime of 2.20 μsec. The spin is associated with a magnetic moment which rotates under a magnetic field with the angular frequency of $2\pi \times 13.55$ kHz/G. Because of its large spin polarization during production and the preferential emission of the positron along the spin direction, we can detect the spin direction of the muon time differentially.

The spin motion of positive muons located at interstitial sites in diamagnetic metals (e.g., Cu, Al) is characterized by the relaxation of spin polarization under random local fields from surrounding nuclear magnetic moments (T_2 relaxation). The spin-relaxation time due to the nuclear magnetic moments, in most cases, lies in a range close to the muons' lifetime (i.e., μsec), which permits its easy observation.

In general, the local magnetic fields felt by a muon are dynamically modulated by the diffusive motion of the muon and/or by the fluctuation of the surrounding moments, which provides another source of spin relaxation (T_1 relaxation). Since the fluctuation of the nuclear magnetic moments is negligibly slow (< 0.01 μsec^{-1}) in diamagnetic metals, the local field modulation is entirely due to the diffusion of the muon, which is reflected in spin relaxation functions. This is the well-known "motional narrowing" effect of NMR (nuclear magnetic resonance). Thus, measurements of the relaxation function of μ^+ spin provide us with information on the diffusion of this light charged particle in metals.

Since a positive muon has a light mass ($\simeq 0.11 \times m_p$: m_p = proton mass), the localized state is considered to be much more extended compared with the case of the hydrogen isotopes (p,d,t) in metals. Consequently, the migration by quantum-mechanical *tunneling* possibly dominates the muon diffusion and gives rise to exotic behavior at sufficiently low temperature. Because of this potentiality, the diffusion of a positive muon in metals has attracted much interest in the field of μSR (muon spin rotation, relaxation, and resonance) for the past 15 years.

It has been conventional that the diffusion is studied by the spin-rotation techniques under a transverse magnetic field (TF-μSR). However, the interpretation of the spin depolarization measured by the TF-μSR is often ambiguous because it is not sensitive to the difference of depolarization mechanisms. Namely, it was not easy in the TF-μSR spectra to distinguish the T_1 relaxation mechanism from that of T_2, because both mechanisms are reflected in a rotation spectrum through a loss of the phase coherence.

Regardless of such an inherent drawback, the first pioneering experiment was performed by Gurevich *et al.* in 1972.[1] In their work and in succeeding work[2] they measured the spin-rotation time spectrum under a transverse magnetic field in copper from 10 to 300 K and analyzed the damping of the polarization (rotation amplitude) $P(t)$ by a simple formula

$$P(t) = \exp\left[-\frac{2\sigma^2}{\nu^2}(e^{-\nu t} - 1 + \nu t)\right] \quad (1)$$

derived from the motional narrowing assumption, where

σ is the relaxation rate in the static limit and ν is the spin-correlation rate interpreted as the diffusion (hopping) rate of the muon.

It was found that if σ was independent of temperature the deduced diffusion (hopping) rate ν was well described by an Arrhenius formula above 100 K, i.e.,

$$\nu = \nu_0 e^{-E_a/kT}, \tag{2}$$

however, the preexponential factor ν_0 ($\simeq 10^{7\sim 8}$ sec^{-1}) and the activation energy E_a ($\simeq 600$ K) in Eq. (2) were too small to be interpreted as arising from diffusion by classical overbarrier hopping. They also found that the muon is almost immobile below 100 K, but could not determine to what extent the muon is mobile because $P(t)$ is insensitive to ν in the slow modulation regime $\nu \ll \sigma$.

The above feature of muon diffusion has been explained by theoretical models based on the small-polaron diffusion theory.[3-6] In these models, the muon is in a small-polaron state and diffuses via so-called incoherent tunneling. In the ground state the muon is localized with the deformation of the host lattice to a lower potential energy than that of the adjacent sites. The tunneling probability is much enhanced when the small-polaron energy levels in the neighboring potential wells become temporarily degenerate due to the modification of the muonic potential by thermally excited phonons. The activation energy E_a in Eq. (2) is interpreted as the energy to realize such a degeneracy of muonic states, which is considerably lower than the energy required to jump over the potential barrier.

It was soon shown by Camani *et al.*[7] and Hartmann[8] that the quadrupolar interaction between the copper nuclei and the electric field gradient (EFG) was important in interpreting the value of σ. The EFG is produced by the muon in an interstitial site. The quadrupolar interaction with such an EFG affects the quantization axis of the surrounding nuclear magnetic moments so that σ increases from the usual Van-Vleck value if the external field is weak ($\gamma_\mu H_0 < eqQ$).[9] The study of the field dependence of σ in single-crystal copper at 20–80 K revealed that the muon occupies octahedral interstitial sites in the above temperature region.[7] They also concluded that a 5% dilatation of the copper lattice around the muon was necessary to explain the absolute value of σ. A theoretical calculation of the potential felt by muons[5] also favors the location of muons at octahedral interstitial sites in copper.

In further TF-μSR investigation the TF relaxation rate was found to decrease again below 5 K.[10-12] If this were interpreted in terms of motional narrowing, it would indicate that the diffusion rate surprisingly increases with decreasing temperature.

However, there have appeared several theoretical models which do not need such a drastic interpretation. For example, the results could be interpreted as a decrease of static width (σ) itself due to the population of a metastable tetrahedral interstitial site below 5 K.[13] This brings us back to what we called the inherent drawback of TF-μSR which makes it difficult to untangle the origin of the depolarization.

With the advent of the zero-field spin-relaxation (ZF-μSR) method,[14-18] it was recognized that more information could be obtained because of its sensitivity to the slow modulation of the local field. The ZF relaxation function has an asymptotic component called the "$\frac{1}{3}$ *tail*" which damps only by the *dynamical* fluctuation of the local field. In diamagnetic metals the existence of the asymptotic component gives a clear signature for the static nature of the local field, and the damping gives the slow hopping rate of the muon itself. This also means that we can determine the static width (σ) of the local field with less ambiguity. Furthermore, the ZF method can discriminate trapping and detrapping processes from single-step diffusion by detailed line-shape analysis.[19,20]

In this paper we shall report in detail on the diffusion of positive muons in copper which was clarified for the first time by the ZF-μSR method. The method immediately provided clear evidence that the change of relaxation rate in TF-μSR at low temperature originates from the diffusive motion of the muon.[21-23] These were followed by our extensive study of ZF-μSR which revealed an exotic temperature dependence for the hopping rate below 20 K as

$$\nu \propto T^{-\alpha}, \tag{3}$$

where α takes small positive number ($\simeq 0.4 \sim 0.6$).[24,25] The temperature dependence was well explained by taking account of the effect of the conduction-electron cloud which at once renormalizes the muon tunneling matrix by a factor $(kT/D)^{2K}$ ($0 < K < \frac{1}{2}$) and reduces the final-state density of muon by $1/kT$, where D is the conduction-electron band width.[26-29]

It is known that TF-μSR is not sensitive to hopping rates smaller than σ, while the sensitivity of the ZF-μSR to the small hopping rate is limited only by the time range available for the observation of the asymptotic component without suffering from background. The pulsed muon beam is most suitable to bring this method into full play, because there is virtually no background, regardless of the beam intensity, which is not true in continuous-beam experiments. For this reason the ZF-μSR has been extensively developed at BOOM (Booster Meson Facility, in KEK, Japan). This paper is one of the first reports of the successful application of the ZF-μSR method with the pulsed muon beam.

In the next section we will give a brief review of the zero- and longitudinal-field (LF) spin-relaxation method. In the succeeding Secs. III–V a full description of our experimental method and results at BOOM will be presented.

II. METHOD

From the view point of taxonomy, the method of μSR is classified by its observables into categories of rotation, relaxation, and resonance. Instead of giving a comprehensive review of these methods,[30] we concentrate on the method of zero-field and low longitudinal field spin relaxation (ZF-, LF-μSR) which are relevant to our

work.[14–18] (The term "longitudinal field" means that the external field is applied along the initial muon-spin direction.)

In the ZF- and LF-μSR methods, one measures the time differential spectrum of decay positrons under a zero or longitudinal magnetic field.[16] The time spectrum $N(t)$ involves the longitudinal spin-relaxation function $G_z(t)$ as

$$N(t)=N_0[1+AG_z(t)]\exp\left[-\frac{t}{\tau_\mu}\right]+B \ , \tag{4}$$

where N_0 is a normalization constant, τ_μ is the muon-decay life time, A ($\simeq\frac{1}{3}$) is the positron asymmetry with reference to the muon-spin polarization, and B is the constant background. Using the above formula, we can extract the spin-relaxation function directly from the measured positron spectrum.

The relaxation function $G_z(t)$ involves two parameters, the dipolar width Δ and hopping rate ν, by which the shape of the relaxation function is virtually determined. In the subsequent sections the physical meanings of these parameters are presented. The level crossing resonance method which has been used in copper recently[31,32] will also be introduced briefly at the end of this section.

A. Zero- and longitudinal-field spin relaxation

The important features of the ZF- and LF-relaxation functions as probes of the spin dynamics is already demonstrated in the formulation of Kubo and Toyabe.[18] Provided that the local field is completely static (i.e., without diffusive motion), the time evolution of the muon's spin $\sigma(t)=[0,0,\sigma_z(t)]$ is described as the motion of magnetic moment under a local magnetic field $\mathbf{B}=(B_x,B_y,B_z)$ as,

$$\begin{aligned}\sigma_z(t)&=\frac{B_z^2}{B^2}+\frac{B_x^2+B_y^2}{B^2}\cos(\gamma_\mu Bt)\\&=\cos^2\theta+\sin^2\theta\cos(\gamma_\mu Bt) \ ,\end{aligned} \tag{5}$$

where γ_μ refers to the gyromagnetic ratio of the muon and θ to the polar angle of $\mathbf{B}$. Suppose that the distribution of static local field is isotropic in direction and approximated by a Gaussian distribution, i.e.,

$$\begin{aligned}&P(B_i)=\frac{\gamma_\mu}{\sqrt{2\pi}\Delta}\exp\left[-\frac{\gamma_\mu^2B_i^2}{2\Delta^2}\right] \quad (i=x,y,z) \ ,\\&\Delta^2/\gamma_\mu^2=\langle B_x^2\rangle=\langle B_y^2\rangle=\langle B_z^2\rangle \ ,\end{aligned} \tag{6}$$

the spin-relaxation function $g_z(t)$ is deduced from the average of Eq. (5) over the local field distribution as

$$\begin{aligned}g_z(t)=\int_{-\infty}^{\infty}\int_{-\infty}^{\infty}\int_{-\infty}^{\infty}&\sigma_z(t)P(B_x)P(B_y)\\&\times P(B_z)dB_x\,dB_y\,dB_z\end{aligned} \tag{7}$$

which yields a relaxation function

$$g_z(t)=g_z^{\mathrm{KT}}(t)=\tfrac{1}{3}+\tfrac{2}{3}(1-\Delta^2t^2)\exp(-\tfrac{1}{2}\Delta^2t^2) \tag{8}$$

called a static Kubo-Toyabe function (see Fig. 1). The time constant Δ is connected directly with the root mean square of the random local field as shown in Eq. (6).

It is clear from the above derivation that the asymptotic component $\frac{1}{3}$ is a residue after the average by the random local field, which comes from the component of the local field parallel with the initial spin direction of muon. This is a quite general consequence of the isotropic randomness irrespective of the detailed form of the distribution function $P(\mathbf{B})$. On the other hand, the initial part of the $g_z(t)(t\le\Delta^{-1})$ is rather dependent on the assumed form of the $P(\mathbf{B})$. For example, if we take a Lorentzian distribution for the $P(\mathbf{B})$, the relaxation shows an exponential damping.

Under a longitudinal external magnetic field $\mathbf{B}_0=(0,0,B_0)$, the relaxation function is derived in the same procedure with a replacement of $P(B_z)$ by $P(B_z-B_0)$ to obtain

$$\begin{aligned}g_z(t)&=g_z^{\mathrm{KT}}(t)\\&=1-\frac{2\Delta^2}{\omega_0^2}[1-\exp(-\tfrac{1}{2}\Delta^2t^2)\cos(\omega_0t)]\\&\quad+\frac{2\Delta^4}{\omega_0^3}\int_0^t\exp(-\tfrac{1}{2}\Delta^2\tau^2)\sin(\omega_0\tau)d\tau \ ,\end{aligned} \tag{9}$$

where $\omega_0=\gamma_\mu B_0$. The asymptotic value of the above relaxation function is always larger than $\frac{1}{3}$.[16]

For the quantitative description of the spin relaxation of a muon in copper, it is necessary to introduce a Hamiltonian to describe the spin motion of the muon ($S=\frac{1}{2}$) interacting with the surrounding nuclei of spin I ($=\frac{3}{2}$ for ^{63}Cu and ^{65}Cu). There are three different interactions in the spin Hamiltonian, the Zeeman interaction under external field denoted as H_0, the magnetic dipole-dipole interaction H_D between the muon and the surrounding nuclei, and the electric quadrupolar interaction H_Q giving the self-energy of the surrounding nuclei (when $I\ge\frac{3}{2}$). The last term is due to the existence of the electric field gradient (EFG) produced from the positive charge of the muon. The spin Hamiltonian is given as

$$H_S=H_0+H_D+H_Q \ , \tag{10}$$

which is to be solved to yield the spin-relaxation function $g_z(t)$.

The static width Δ is calculated by the following equation:

$$2\Delta^2=-\frac{\mathrm{tr}\{[\bar{H}_D,S_z]^2\}}{\mathrm{tr}[S_z^2]} \ , \tag{11}$$

where $\bar{H}_D$ is from residual terms of H_D (called *secular* terms) when H_0 or H_Q dominates. Since the dipole-dipole interaction decreases rapidly with the distance r as $1/r^3$, the second moment is dominated by the nuclei at the nearest-neighboring sites.

In the case of zero or low external field, it is not easy to get the relaxation function directly by solving Eq. (10) to a good accuracy because the term H_D or H_Q cannot be treated as a perturbation. Even in such cases the second moment can be predicted from a semiclassical argument as to which component of the random local field contrib-

utes to the spin relaxation of muon. For detailed discussions of Δ^2, see Refs. 16 and 17.

An attempt to calculate a more realistic relaxation function has been attained by solving numerically the quantum-mechanical equation of motion for Eq. (10) with a finite number of nuclei.[33–37] As shown in Fig. 1 by a solid curve, the calculated relaxation function shows a small ($\sim 5\%$) oscillatory deviation from Eqs. (8) and (9). In classical terminology the deviation is considered to come mainly from the difference of the local field from a Gaussian distribution. The difference will be discussed in Sec. IV A 1 in detail.

The effect of muon diffusion on $G_z(t)$ is approximated by a stochastic model for the time evolution of a local field by the migration of a muon under a Markovian process (strong collision model).[38,39,16,40] The relaxation function is described in the form of an integral equation as

$$G_z(t)=g_z(t)e^{-\nu t}+\nu\int_0^t g_z(\tau)e^{-\nu\tau}G_z(t-\tau)d\tau\ , \qquad (12)$$

where $\nu^{-1}\equiv\tau_c$ is the spin-correlation time whose reciprocal is interpreted as the hopping rate. The diffusion coefficient D_μ of a muon in copper is related to the hopping rate as $D_\mu=1/za_0^2\nu$ under the assumption that a muon hops between neighboring sites, where a_0 is the lattice constant and z is the coordination number ($z=12$ for octahedral interstitial sites). Typical examples of $G_z(t)$ are shown in Fig. 1 calculated from the above equation with the function of Ref. 37 for $g_z(t)$.[41]

In the slow-modulation regime ($\nu\leq\Delta$), the asymptotic $\frac{1}{3}$ tail of the Kubo-Toyabe function (ZF) exponentially damps as[16,15]

$$G_z(t)\simeq\tfrac{1}{3}\exp(-\tfrac{2}{3}\nu t)\quad(t\gg\Delta^{-1})\ , \qquad (13)$$

while in the fast diffusion ($\nu\gg\Delta$), it is approximated in another exponential damping form as

$$G_z(t)\simeq\exp\left[-\frac{2\Delta^2 t}{\nu}\right]\quad(\nu\ll\gamma_I B_2,\omega_Q)\ . \qquad (14)$$

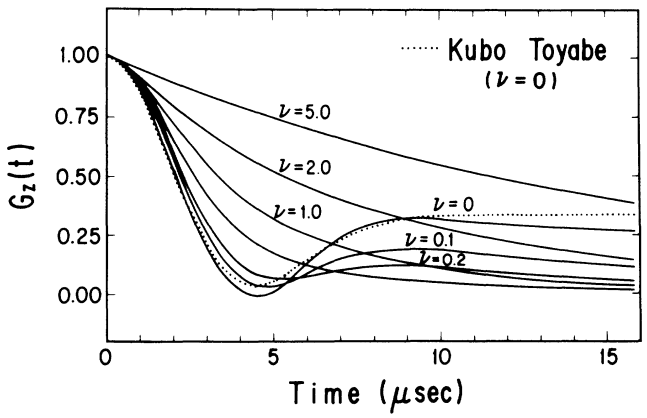

FIG. 1. Zero-field longitudinal spin-relaxation function (the original static relaxation function by Celio) calculated for several different cases of hopping rate ν by strong collision model (ν is normalized by $\Delta=0.39\ \mu\text{sec}^{-1}$).

One important character of Eq. (13) is that it does not depend on the local field parameter Δ, while Eq. (14) does. Note also that in Eqs. (13) and (14) the effects of the hopping rate ν are converse to each other. Since the latter is called "*motional narrowing*" in NMR, the former effect may be called "*motional broadening*" as a general phenomena in ZF- and LF-μSR.

The coefficient of νt ($=\frac{2}{3}$) in Eq. (13) is interpreted as the fraction of polarization which depolarizes at every hop. This is due to the fact that muon is assumed to feel an uncorrelated local field after migration in the Markovian process. It is known that the coefficient is different under different assumptions of the stochastic process for the migration. Assuming a Gaussian-Markovian process in deriving the time evolution of the local field, Kubo *et al.* found the coefficient to be about 1.56 instead of $\frac{2}{3}$.[42] So far there is no experimental study to distinguish them.

Practically, the observable time range may not be long enough for the asymptotic component to be observed clearly. In such a case the slow modulation of the local field can be studied by the low-longitudinal-field (LLF) spin-relaxation method.[16,41] As shown in Eq. (9), $g_z(t)$ under LLF converges more rapidly to the asymptotic value with enhanced amplitude compared with the zero-field case. Assuming a Markovian process, the damping of the asymptotic component in the slow-modulation regime ($\nu\leq\Delta$) is

$$G_z(t)\simeq g_\infty\exp[-(1-g_\infty)\nu t]\ ,$$
$$g_\infty=g_z(\infty)\ . \qquad (15)$$

The above equation indicates that the optimum condition for the LLF method is that the field is chosen to satisfy $g_\infty=\frac{1}{2}$ which corresponds to $B_0\simeq 1.23\Delta/\gamma_\mu$.

The relaxation function under various longitudinal fields can tell us whether the muon motion is a single-step process or a trapping-and-detrapping process.[19] For example, suppose that the muon has a metastable state where the dipolar width takes a different value $\Delta_m<\Delta$. As shown in Fig. 2, if the lifetime of the metastable state is long enough compared with Δ^{-1}, the zero-field time spectrum resembles the fast-modulated spectrum with a single Δ. However, these two cases are easily discriminated by applying the longitudinal field. Namely, if there is fast modulation, the longitudinal field does not suppress the observed depolarization.

Finally, we comment on the choice of the zero-field relaxation function $g_z(t)$ for data analysis. Early ZF-μSR experiments were analyzed using a Kubo-Toyabe function for $g_z(t)$ which assumes a Gaussian distribution of the local field. Good agreement within the statistical accuracy was obtained.[21–24] Recently, the ZF relaxation function was examined in a high statistics measurement,[35] and experimental data were found to fit better with a function calculated by Holzschuh and Meier for the quantum-mechanical system of a muon and the nearest-neighboring copper nuclei.[36] The theoretical situation has been further developed by Celio.[37] Both the

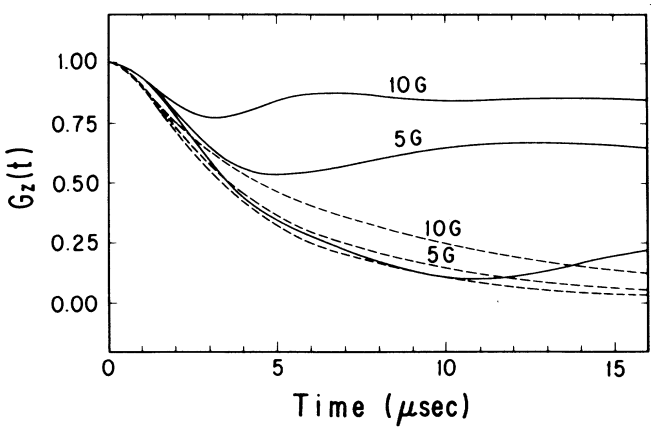

FIG. 2. Low-longitudinal-field spin-relaxation functions at 0, 5, 10 G ($\Delta=0.39\ \mu\text{sec}^{-1}$). Solid line: $\Delta_m/\Delta=0.42$, $\nu=0$ and assuming that a $\frac{1}{3}$ fraction of muons occupies the Δ_m site (e.g., considering the case of tetrahedral interstitial sites for the metastable site). Dashed line: single Δ with fast hopping ($\nu\sim\Delta$).

Kubo-Toyabe function and the Celio function were used for the present analysis to check the validity of the previous result.

B. Level crossing resonance

The application of the level-crossing resonance method to μSR was proposed quite recently,[31] and the first successful resonance was found in a μSR experiment in copper.[32] In general LCR is considered to be a resonant transfer of the energy or entropy between the two ensembles which have discrete energy levels and are weakly coupled together by some appropriate interaction. Provided that one of them is initially in a nonequilibrium state with others, the coincidence of the energy splitting of these two systems enhances the energy transfer between them to equilibrate these two systems.

In the case of a muon in copper, as shown in Fig. 3, the polarization transfer occurs between muon and surrounding copper nuclei when the muon Zeeman splitting $\hbar\omega_\mu$ by H_0 coincides with the quadrupole splitting of copper nuclei $\hbar\omega_Q$ by H_Q [see Eq. (10)]. [More specifically, the degeneracy as to I_z (nuclear spin $I=\frac{3}{2}$) in H_Q is removed due to the nuclear Zeeman interaction in H_0.] Thus, if $H_D \ll H_Q$ is satisfied, we can drive a resonance spectroscopy by changing the width of the muon Zeeman splitting. The resonance is observed as an enhancement of the muon-spin depolarization due to the spin flip of the muon by the dipolar interaction H_D.

Since the electric field gradient at the copper nuclei is produced by the muon itself, the LCR is expected to be very sensitive to a change of muon location in the crystal. In TF-μSR the field dependence of the dipolar relaxation rate $\sigma(B)$ in single-crystal copper is dependent on the symmetry of the interstitial site around the decoupling field ($\gamma_I B\sim\hbar\omega_Q$), which also gives us information on the location of muon.[7,8]

As we show in the following, the LCR effect is already implicit in the formulation of relaxation function in Ref.

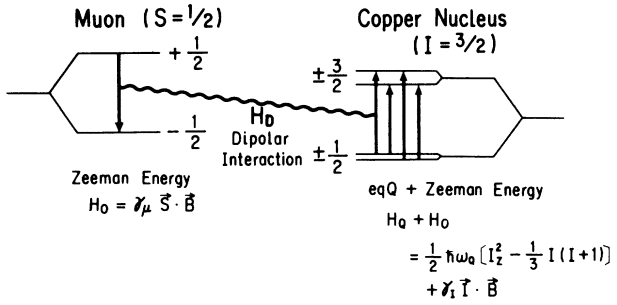

FIG. 3. Level scheme of the muon level crossing resonance in copper: Energy transfer occurs between muonic Zeeman energy level and nuclear electric quadrupolar (eqQ) energy level through magnetic dipolar interaction, which causes a spin flip for both systems.

16. The relaxation functions deduced through the formulation of Kubo and Tomita[43] are as follows:

$$G_z(t)=\exp[-\Psi_z(t)]\ , \tag{16}$$

$$G_x(t)=\exp[-\Psi_x(t)]\ ,$$

$$\Psi_z(t)=\tfrac{1}{2}\phi_0 g_\nu(\omega_\mu-\omega_I,t)+\phi_1 g_\nu(\omega_\mu,t)+\phi_2 g_\nu(\omega_\mu+\omega_I,t)\ , \tag{17}$$

$$\Psi_x(t)=\phi_0 g_\nu(0,t)+\phi_1 g_\nu(\omega_I,t)+\tfrac{1}{2}\Psi_z(t)\ ,$$

$$g_\nu(\omega,t)=\text{Re}\left[\frac{e^{-\nu t}e^{-i\omega t}-1+(\nu-i\omega)t}{(\nu-i\omega)^2}\right]\ ,$$

where $\omega_{\mu,I}=\gamma_{\mu,I}B_z$ and ϕ_0,ϕ_1,ϕ_2 ($\sim|H_D|^2$ in order of magnitude) are constants dependent on the geometrical configuration of the host nuclei with respect to the muon.

Let us consider the case of the longitudinal spin-relaxation function $G_z(t)$. The function $G_z(t)$ shows damping from 1 when $\omega\sim0$ is satisfied. If we can neglect the nuclear Zeeman energy [i.e., $O(\gamma_I/\gamma_\mu)\ll1$: $\gamma_{\text{Cu}}/\gamma_\mu\simeq0.085$ for ^{63}Cu], ω_I can be replaced by ω_Q and the coincidence between $\pm\omega_\mu$ and ω_Q satisfies the resonant relaxation condition to cause the damping of $G_z(t)$. In this case the function $g_\nu(\omega,t)$ is approximated as

$$g_\nu(0,t)\simeq\frac{e^{-\nu t}-1+\nu t}{\nu^2}\ , \tag{18}$$

which corresponds to Eq. (1) (Abragam formula). Thus in the case of slow hopping, for instance, $G_z(t)$ has a Gaussian-like damping with rate $\simeq(\phi_0)^{1/2}/2$ ($\omega_\mu=\omega_Q$) or $(\phi_2/2)^{1/2}$ ($\omega_\mu=-\omega_Q$) on resonance. A similar effect is also found in the case of the transverse spin-relaxation function $G_x(t)$.

The effective relaxation rate is determined by the average over geometrical configurations of nuclei contributing to the resonance. To clearly see the resonance of the relaxation rate, the quadrupolar interaction should be strong enough to satisfy $\phi_{0,2}\ll\omega_Q^2$. The Zeeman splitting of the muon energy level is smeared out by the muon-nuclear dipolar interaction H_D, which determines the width of the resonance. Thus the resonance curve for

LCR is expected to reflect the distribution of local magnetic fields.

To give a schematic idea of the LCR spectrum some examples of calculated relaxation functions by Eq. (16) are shown in Fig. 4. In this calculation we assumed $\phi_0=\phi_1=\phi_2$ ($\simeq\Delta$) and $\omega_\mu/\gamma_\mu\Delta\sim 18$ to simulate the case of LCR in copper. It is clear from $g_v(0,t)$ that the hopping of the muon causes the usual motional narrowing for the LCR time spectrum. However, as shown in Fig. 4, it should be emphasized that the presence of hopping does not result in the motional narrowing of the resonance width but causes a reduction of resonance amplitude. It is interesting to note that there is some structure (bump) in the field dependence of $G_z(t)$ around the resonance region in Fig. 4(b). Thus, we should be careful about the interpretation of LCR spectrum under the presence of dynamic effects. A more complete discussion of LCR spectra will be found in Refs. 37 and 44.

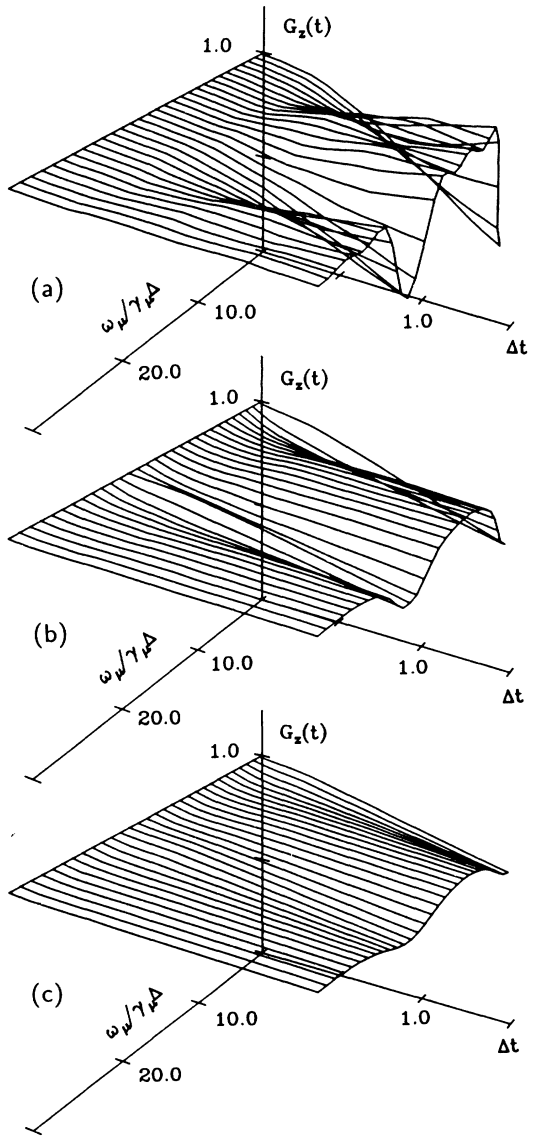

FIG. 4. Longitudinal relaxation function $G_z(t)$ calculated by Kubo-Tomita formula as a function of applied longitudinal magnetic field ω_μ (see text for details). The parameters of the function were chosen to simulate the case of muon in copper: $\omega_I/\gamma_\mu\Delta\simeq 18$, $\phi_0=\phi_1=\phi_2$ ($\simeq\Delta$). Hopping rate ν was chosen as (a) $\nu/\Delta=0$, (b) $\nu/\Delta=2.0$, (c) $\nu/\Delta=4.0$, respectively.

III. EXPERIMENT

A. Muon beam

A very important methodological feature of the present work is the use of a *pulsed muon beam* which is provided by the Booster Meson Facility (BOOM) (Ref. 45) at KEK. The beam has a sharply pulsed time structure of 50 nsec width coming at a rate of 20 Hz, which is due to the beam structure of the booster proton synchrotron. One proton beam pulse produces about 10^3 muons (per pulse) available for the experiment for a primary proton current of $2\sim 4$ μA. The time origin of the μ-e decay measurement is determined by the arrival time of the muon beam. On the other hand, in a continuous (dc) beam experiment, muons come randomly in time. Their arrival is identified one by one by a set of muon counters. For the time-differential measurement of μ-e decay in a long time range, the pulsed muon beam has the following characteristics, superior to the dc muon beam.

In experiments using a continuous muon beam there is a background arising from accidental coincidence between a stopped muon event and a decay positron event or a possible background positron which is not necessarily associated with muon decay. The accidental coincidence rate is essentially determined by the muon stopping rate, time range of the decay positron measurement, and the positron detection rate. This background puts a serious limit on the time range for a μ-e decay measurement with the dc muon beam. The pulsed muon beam is free from such background. The main background comes from neutrons generated at the pion-production target and beam dump. The typical background rate is about 10^{-4} or less of the μ-e decay counting rate at the time origin. This means that we can extend the time range of measurement to $2.2\times\ln 10^4\simeq 20$ μsec. Compared with the pulsed beam, the dc muon beam has more than 100 times larger background under the usual conditions.

More generally, in a time-differential measurement, if we could measure multiple μ-e decay events without distortion, the pulsed beam would put no restriction on the incoming number of muons. In the case of a dc beam, the incoming rate is limited by the time range of interest for the μ-e decay measurement because of the accidental background.

However, in the present experiment there are some disadvantages to using a pulsed muon beam. One is that it is difficult to distinguish the muon stopping in the relevant target from that stopping in the surrounding materials; this produces background μ-e decays. Thus the signal-to-noise ratio of the μ-e decay measurement is determined by the ratio of the muon stopping events between the target and the surrounding materials. To avoid serious contamination by such an unwanted μ-e decay,

we must prepare a target of large enough cross section and thickness to reduce the relative number of muons which stop in the surroundings. In addition, to be free from the distortions in the time spectrum the choice of the surrounding material is important. Namely, we should avoid any material in the surrounding equipment such as cryostats for which the muon shows unexpected relaxation.

Another problem is that phenomena occurring in a time shorter than the beam pulse width (50 nsec) cannot be measured. This is in marked contrast to the case of a dc beam, where there is no principal restriction to the time resolution of the measurement. In the case of the present study, however, the spin relaxation of muons in copper is slow enough that the finite beam width causes no problem.

The present experiment was performed mainly at the $\mu 1$ port at BOOM using the backward muon beam produced from pion decay in flight inside a superconducting solenoid ($\simeq 6$ m). The beam momentum 75 MeV/c was chosen to maximize the muon stopping rate. The muons have about 80% spin polarization along the beam momentum direction. The beam spot size is roughly 6 cm$\times$6 cm. Part of the measurements were done at the $\pi 1$ port using the muon beam (29 MeV/c) produced from the pion decay near the surface of the production target. The contaminating positrons in this muon beam were eliminated by a static electric field ($\simeq \pm 70$ kV). The beam spot size is roughly 3 cm$\times$3 cm.

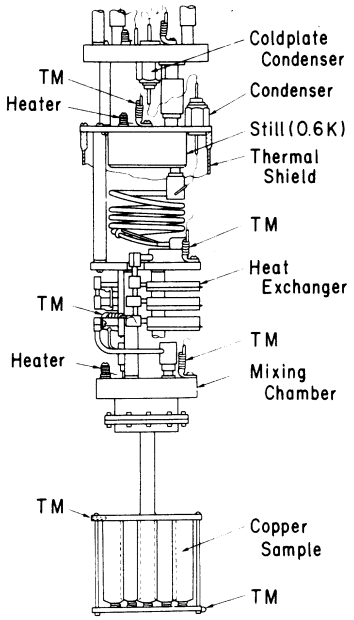

FIG. 5. Copper sample mounted in a dilution refrigerator. The picture displays the configuration for sample A (five rods of the highest purity copper). The rods are held between metal plates made of copper and aluminum, connected to the bottom of the mixing chamber through a 10-mm ϕ copper rod. TM stands for a resistance thermometer.

B. Copper samples

Three copper samples of different purities were prepared at Institut für Festkörperforschung, Kernforschungsanlage, Jülich, Germany for the present experiment. The specific features of these samples are summarized in Table I. The detailed description as to the preparation of these samples is given in Ref. 12.

As noted in the previous section, the dimension of the sample is important when using a pulsed muon beam. In order to stop the incoming muon efficiently, the thickness of the sample should be larger than the muon range width coming from the beam momentum spread. The measured muon stopping range at 75 MeV/c is about 4 g/cm^2 with a range width of 3 g/cm^2 (FWHM).

Six different target sample holders were fabricated for the present experiment. One of these configurations is shown in Fig. 5. The cross section of the sample holders seen from the muon beam is designed to be as small as possible. In addition, all of these holders are made from 99.99% pure aluminum where no significant spin relaxation of muon is anticipated.[10,46]

C. Target surroundings

The experimental apparatus consists of a liquid-helium cryostat for the target sample (copper), a beam collimator, positron counters, and Helmholtz-type coils for longitudinal and transverse magnetic fields. A helium-gas-flow-type cryostat (Oxford Institute Model No. CF-104) was used for the measurement at temperatures higher than 4.2 K. Below 4.2 K, a ^{3}He-^{4}He dilution refrigerator (S.H.E. Model No. DRI-420) was installed. A schematic view of the apparatus for the dilution refrigerator (side view) is shown in Fig. 6. We shall concentrate on the layout of the apparatus for the dilution refrigerator in the following.

All the samples in the dilution refrigerator were cooled by thermal conduction from the "mixing chamber" (see Fig. 5). The holders were designed to have enough thermal conductivity at 10$\sim$100 mK to avoid a thermal gradient between the sample and mixing chamber.[47] The samples A and B were attached to the mixing chamber through a copper rod (10 mm ϕ) and appropriate holders.

The temperature of the sample was monitored by two

TABLE I. Summary of the data for the copper samples. RRR refers to the residual resistivity ratio.

Sample	Purity	Dimension (mm)	T range
Copper A	RRR = 18 000	$13\phi \times 50 \times 5$ rods (~ 10 g/cm^2)	0.07–190 K
Copper B	RRR = 7350	$8t \times 60 \times 50$ (~ 7 g/cm^2)	0.07–140 K
Copper C	95 at. ppm Fe	$6t \times 60 \times 40$ (~ 5 g/cm^2)	0.1–8 K

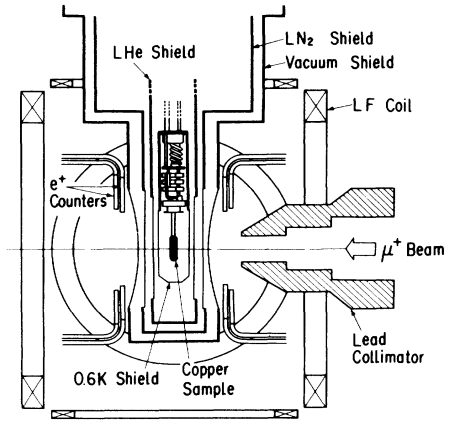

FIG. 6. A cross section of cryostat for dilution refrigerator. All the walls along the beam pass have windows made of thin metal foil or mylar sheet. Sixteen positron telescope counters are assembled coaxially around the beam axis for both upstream (≡backward) and downstream (≡forward) sides coming with the muon beam.

carbon-resistance thermometers below 4.2 K and by two thermocouples above 4.2 K. These were mounted on the top and the bottom of the sample and the average of both thermometers was defined as the temperature of the sample. The fluctuation of the temperature was typically about 3% below 4.2 K and 1% above 4.2 K throughout the measurement.

As shown in Fig. 6 the target and the main part of the dilution refrigerator are covered with a thermal shield made of 100-μm-thick copper extended from the "still" ($\sim$0.6 K). The next two layers are the 4.2-K (liquid-helium) and 77-K (liquid-nitrogen) thermal shields. These shields are both made of aluminum and have large windows of 100-μm-thick aluminum foils for the muon beam to pass through. The outer-most vacuum shield is made of SUS-304 which has windows of 28 cm diam covered with 100-μm-thick mylar sheet.

The positron telescopes are assembled around the cryostat as shown in Fig. 6. A telescope consists of a pair of plastic scintillation counters. The signal from each counter is led to a photomultiplier through a flexible light guide made of optical fiber. Sixteen telescopes are cylindrically mounted on each side of the cryostat, covering the total solid angle of about 10%. The typical μ-e decay event rate was 30$\sim$40 events/pulse for the backward (upstream) 16 telescopes and 60$\sim$70 events/pulse for the forward (downstream) 16 telescopes. The difference of the event rate between two groups of telescopes is due to the events concentrated at the origin of the time spectrum, probably due to the positron contamination in the beam. The backward telescopes are protected from such a background by a lead collimator, yielding better time spectra. The distortion of the time spectrum will be discussed in a later section.

The system has two pairs of Helmholtz-type coils to generate both longitudinal and transverse magnetic fields. Although the configuration of the coils does not satisfy the exact Helmholtz condition, the inhomogeneity of the field is less than 5% within the target volume. In addition, three pairs of small coils were installed to cancel the leakage field from other experimental equipments. The residual magnetic field under zero-field condition was less than 0.3 G for any direction throughout the measurement.

D. Data acquisition

The data acquisition of the μ-SR experiment for a pulsed muon beam is considerably different from that for a continuous beam. Namely, the acquisition system must have an ability to accept multiple μ-e decay events following one muon beam pulse. There are two essentially different methods for resolving this problem. One is to develop a multistop time-to-digital converter (TDC) (Ref. 48) and the other is to use the analog signal of the positron counter.[49] For the present experiment the former method was used because of its reliability at the stage of the present experiment.

In the case of applying a multistop TDC, it is important that the time bin of the TDC is short enough to distinguish two successive events in a telescope; otherwise a distortion of time spectrum arises due to the counting loss. Since the μ-e decay follows a Poisson distribution, the pile-up probability that two or more μ-e decay events occur within a time bin d is written as,

$$P_{n\geq 2}=\frac{1}{P(1)}\sum_{k=2}^{\infty}P(k)\ , \tag{19}$$

where

$$P(n)=\frac{r^n e^{-r}}{n!},\quad r\simeq\frac{dm}{\tau_\mu}e^{-t/\tau_\mu}\ ,$$

and m refers to the expected μ-e decay event number per pulse, τ_μ to the muon-decay lifetime. In the case of small r, Eq. (19) is approximated by

$$P_{n\geq 2}=\frac{r}{2}\simeq\frac{dm}{2\tau_\mu}e^{-t/\tau_\mu}\ . \tag{20}$$

In the case of the present experiment the time bin d is 16 nsec, and assuming that all the detected events come from μ-e decay, we estimate the probability $P_{n\geq 2}$ to be about 0.7% for the rate of 30$\sim$40 events/pulse. It is clear that a shorter time bin with a smaller solid angle of telescope is desirable for the reduction of the pile-up probability.

A schematic view of the data acquisition system is shown in Fig. 7. In each telescope the signals from two photomultipliers (PM's) are discriminated and the coincident signal of the PM's is fed into a multistop TDC. The TDC developed by Shimokoshi *et al.* in our laboratory[48] has an internal memory (2048 words) in which the positron decay time spectrum is automatically accumulated.

The contents of the TDC memory are transferred to the host computer (DEC, VAX-11/780) through a pro-

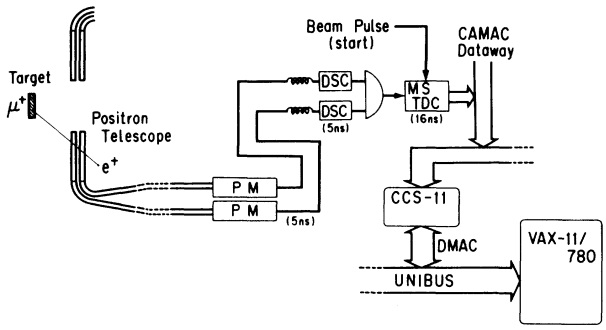

FIG. 7. A schematic view of data flow. PM stands for photo-multiplier, DSC for signal discriminator, and MS TDC for the multistop TDC. Inside the bracket shows time resolution at each point.

grammable CAMAC crate controller (Mitsui Co. Ltd., CCS-11) every 500 beam pulses. The controller was designed and developed by Hayano and is a high speed and flexible data acquisition system.

E. Data analysis

1. *Correction of the time spectrum*

Provided that there is no instrumental error throughout the measurement, the time-differential counting of the decay positron $N(t)$ is written as shown in Eq. (4) (see Sec. II). However, before applying the formula to the data analysis, we have to take into account the possible distortion of the real spectrum. As discussed in the section on data acquisition, the finite probability of pile-up of the positron events results in a reduction of the detection efficiency (which we shall call counting loss). If the number of events per time bin per burst is much less than 1, the practically observed time spectrum $\bar{N}(t)$ is related to the true $N(t)$ by

$$\bar{N}(t)=n_p[1-P(0)] =n_p\left[1-\exp\left[-\frac{N(t)}{n_p}\right]\right], \tag{21}$$

where n_p refers to the total number of the beam pulses taken for a spectrum. We should note that the dead time of the electronic circuits such as coincidence circuit or discriminator causes the same effect. In order to find $G_z(t)$ we invert Eq. (21) to get

$$N(t)=-n_p\ln\left[1-\frac{\bar{N}(t)}{n_p}\right]. \tag{22}$$

The correction of the counting loss was performed by Eq. (22) in advance of the analysis by Eq. (4). The difference of the spectrum before and after the correction is typically 1%, which is not totally negligible. Because of the larger time bin of the TDC in the earlier measurement (i.e., 50 nsec),[23,24] the distortion due to the counting loss was found to be serious, especially for the data around 10~100 K. The measurement for the sample B was repeated again from 10 to 170 K with a shorter time bin (16 nsec) and the old data in this temperature region have been replaced by the new result.

Since the time spectrum showing little damping is sensitive to the distortion at the initial time region, the validity of the correction can be examined by the analysis of the LF spin-relaxation time spectrum. As shown in Fig. 10, the agreement between the corrected spectra and the theoretical function is quite satisfactory.

In addition to these points, we did not use the initial part of the time spectrum (up to ~0.3 μsec) for the final analysis because of the distortions due to the beam prompt. It was found that the initial part of the forward counter's spectrum (~1 μsec) suffered from considerable distortion. This is probably due to the dead time of the photomultiplier caused by the large quantity of light produced by muons *stopped* in the scintillation counters. Therefore only the spectrum from backward counters was used in the final analysis.

2. *Fitting procedure*

After the corrections of the time spectrum, the data were analyzed by Eq. (4) using a χ^2 minimization method (called MINUIT) to deduce the best-fit parameters in Eq. (4).[50,51] The errors of deduced parameters were analyzed by a code called MINOS which determines the error of a parameter by searching the contour of the χ^2 to find the variance of the parameter for which χ^2 increases by 1.0 from the best-fit value. Assuming that the distribution of the deviation of the χ^2 from the best-fit value follows the χ^2 distribution for one degree of freedom for one variable parameter in question, the above definition of the error in MINOS corresponds to the variance of the parameter with 68% confidence level.

IV. RESULTS

A. Pure copper

1. *Comparison of the zero-field spin-relaxation functions: static local field*

We have previously reported an observed oscillatory zero-field $G_z(t)$ at 15 K.[35] The analysis favored a relaxation function calculated by Holzschuh-Meier[36] compared with that of Kubo-Toyabe function. Because an improved calculation of the zero-field relaxation function has been carried out by Celio,[37] let us examine this problem again.

The calculation in Ref. 36 was obtained for a reduced system of a muon and six neighboring copper nuclei under the assumption that the electric quadrupolar interaction is much larger than the magnetic dipolar interaction (i.e., $H_Q \gg H_D$) in the nuclear Hamiltonian, which was not self-evident at that moment. In Ref. 37 the exact strength of H_D and H_Q (and H_0 for the longitudinal field) was taken into account by a new method.

The strength (coupling constant) of the electric quadru-

polar interaction was experimentally determined with less ambiguity by the LCR measurement in copper (at 20 K) from the resonance field $B_{\rm res}$;[32]

$$B_{\rm res}=80.9\pm0.4\ \text{G}\ . \tag{23}$$

If we neglect the small disturbance of the Zeeman interaction on the nuclear energy level, ratio of H_Q/H_D is

$$\frac{H_Q}{H_D}\simeq\frac{\gamma_\mu B_{\rm res}}{\Delta}\simeq\frac{6.85\times10^{-6}\ \text{sec}^{-1}}{0.39\times10^{-6}\ \text{sec}^{-1}}\simeq18\gg1\ . \tag{24}$$

Thus the assumption taken in Ref. 36 is proved to be valid in the case of muon in copper. (The value of the Δ will be discussed later.) Actually, when we adopt the above value for the strength of the H_Q, the resultant relaxation function calculated by the method in Ref. 37 scarcely differs from that by Holzschuh and Meier.

In any case, the primary difference between the calculation of Kubo-Toyabe and other calculations consists of the difference of the shape of the effective local magnetic field. If the influence of the nuclei other than the neighboring ones on the muon is negligible, the result of Ref. 37 indicates that the Gaussian distribution taken in Eq. (6) is not accurate enough for a precise determination of a slow hopping rate. An estimation shows that the effect of the second-nearest-neighboring nuclei is observable only for the time region beyond 15 μsec.[37]

As already shown in the previous result of ZF-μSR experiment in copper, muons are almost immobile between 10$\sim$100 K where the spin relaxation is predominantly determined by the static local magnetic field. Thus, this temperature region is most suitable for a ZF-μSR study of the shape of the local magnetic field.

We performed a comparative analysis of the time spectrum obtained by the recent measurements in the temperature range 40$\sim$80 K using Celio and Kubo-Toyabe functions. As shown in Fig. 8(a), the spectrum dips below and then exceeds the best-fit Kubo-Toyabe function at 4$\sim$5 μsec and 7$\sim$10 μsec, respectively, while the Celio function shows better agreement as a whole. The result of the fitting analysis is shown in Table II. From this result we finally conclude that the local magnetic field seen by muon in copper deviates slightly from the Gaussian distribution and that the spin relaxation is best approximated by the Celio function.

Several examples of the observed time spectra under zero and longitudinal field are shown in Figs. 9 and 10, where the normalized asymmetric part $G_z(t)$ is plotted with the best-fit curve of the Celio relaxation function.[37,41] In the final analysis the asymmetry A for these data was fixed to the average of the values obtained from the data of 10$\sim$100 K. In Fig. 9 the spectrum at the middle temperature (80 K) shows an undamped asymptotic tail, while at the lower and higher temperatures the spectrum shows exponentiallike damping from motional narrowing; see Eq. (14).

The spectra taken with low longitudinal field (LLF) (Fig. 10) show excellent agreement with the theoretical curve in Ref. 37. This result not only ensures again the validity of the assumptions made for the calculation in Ref. 37, but also is evidence against the diffusion-limited trapping model;[19] although we can fit the zero-field spectrum by such a model with appropriate adjustment of the parameters in Eq. (4), the field dependence is clearly different from the prediction of the model assuming simple static relaxation. Such a case is shown in Fig. 10 by dashed curves calculated for the case of 1.3Δ for the dipolar width and $\nu=0.2\Delta$, where the values of the parameters were taken to reproduce the experimental result.

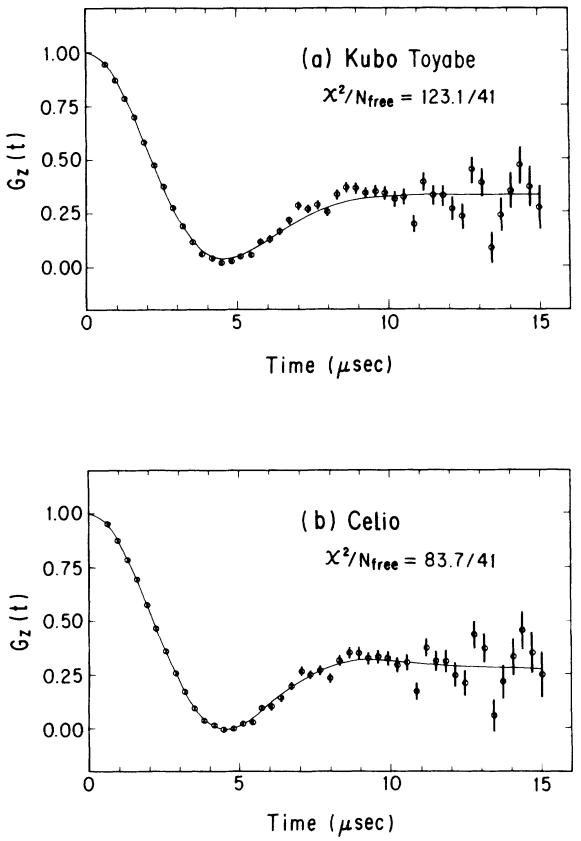

FIG. 8. Comparative analysis of zero-field spin-relaxation time spectrum. The data at 40$\sim$80 K are summed and analyzed by both (a) Kubo-Toyabe and (b) Celio functions. The width of time bin is 0.32 μsec. The resultant χ^2 values (χ^2) and degree of freedom ($N_{\rm free}$) for the fitting analysis are shown.

TABLE II. Parameters and χ^2 values deduced from the comparative analysis of time spectrum at 40–80 K by both Kubo-Toyabe and Celio function. Δ and ν refer to the dipolar width and hopping rate, respectively. The time spectrum was analyzed from 0.63 μsec to 15.3 μsec.

Parameters	Kubo-Toyabe	Celio
A	−0.1643(7)	−0.1592(6)
Δ (μsec^{-1})	0.379(1)	0.383(1)
ν (μsec^{-1})	0.000(6)	0.000(3)
$\chi^2/N_{\rm free}$	123.1/41	83.7/41

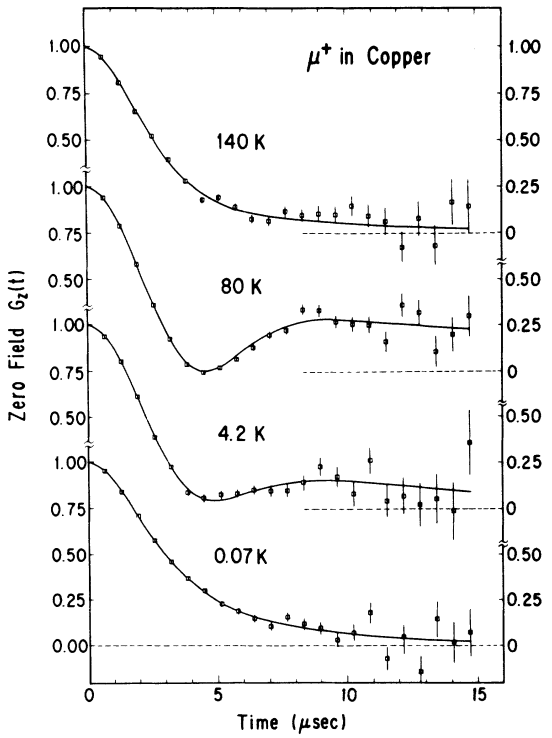

FIG. 9. Examples of the observed time spectra at typical temperature. The asymmetric part is extracted from the positron time spectrum. The solid curve indicates the best fit by Celio function.

2. *Dipolar width and hopping rate*

As noted in the Introduction of this paper, the results reported in the previous papers were obtained using the Kubo-Toyabe relaxation function for $G_z(t)$.[21–25] We analyzed all the spectra using the Kubo-Toyabe function and the Celio function to see how the difference of the relaxation function affects the deduced values of the parameters.

The dipolar width Δ and hopping rate ν are shown in Fig. 11 deduced from the analysis using (a) Kubo-Toyabe function and (b) Celio function for $G_z(t,\nu)$, respectively. The difference in the hopping rate between (a) and (b) is noticeable around the region where muon is static (i.e., showing slow hopping). This is mainly ascribed to the difference of the shape of the asymptotic tail between both relaxation functions. Namely, as seen in Fig. 8, the fit by the Celio function requires larger relaxation rate to reproduce the same relaxation shape because of the larger amplitude of the asymptotic component compared with

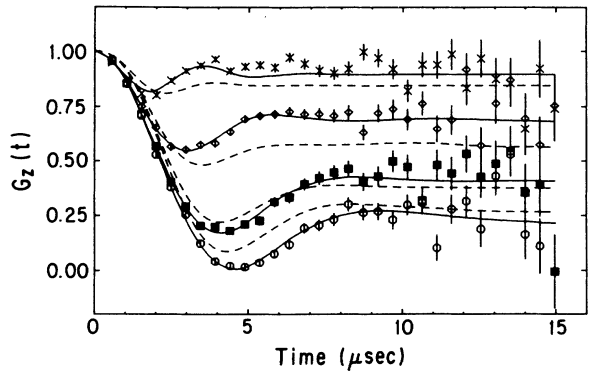

FIG. 10. ZF and LF spin-relaxation function of positive muon in copper at 50 K (30 K for ZF). The data at 0, 5, 10, and 20 G are shown, respectively, with best-fit curves calculated by Celio. The dashed curves show the ZF and LF relaxation functions under the diffusion-limited trapping model with appropriate parameters.

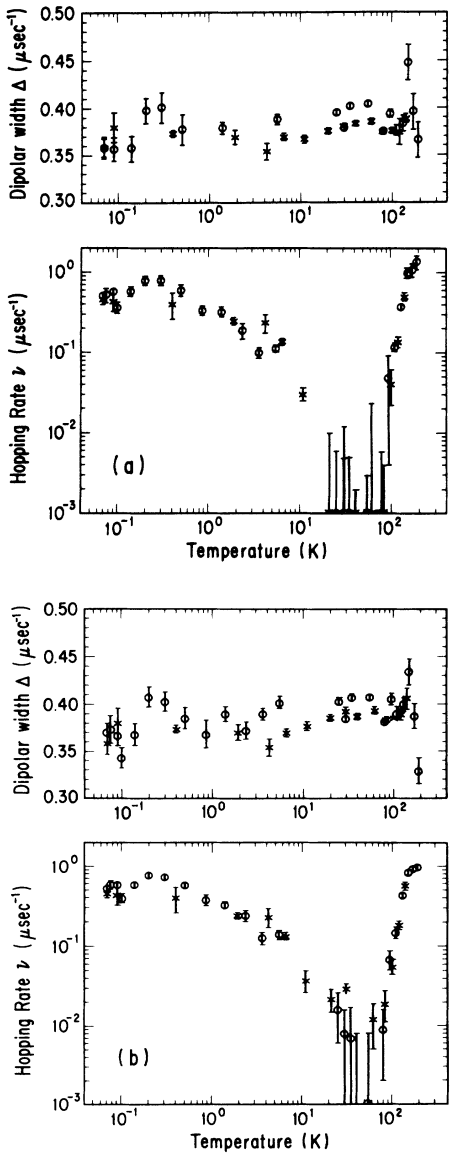

FIG. 11. Results of the analysis by both (a) Kubo-Toyabe function and (b) Celio function. Open circle is copper *A* (RRR is 18 000); Andrew cross is copper *B* (RRR is 7350). The difference is not significant except the static region (10–100 K).

that of the Kubo-Toyabe function. Since we know already that the fit by the Celio function shows a better agreement with the data in the static region, we adopt the result shown in Fig. 11(b).

The result clearly indicates that the dipolar width Δ is independent of temperature from 0.07 to 190 K within the error. This implies that the location of a muon in copper is also temperature independent here. The weighted average of Δ is 0.390 ± 0.001 μsec^{-1} for sample A and 0.386 ± 0.001 μsec^{-1} for sample B, both of which were deduced from the analysis using the Celio function [Fig. 11(b)]. Here, the dipolar width of the Celio function is determined by the initial damping of the numerically calculated function ($0\leq\Delta t\leq0.7$). The agreement of Δ is quite satisfactory between samples A and B.

As shown in Fig. 11, the difference of the hopping rate between samples A and B is not significant in the whole measured temperature region except 0.1–0.5 K where a small bump of the hopping rate is seen in the case of sample A. The bump is, however, correlated with the bump of the dipolar width. Since the parameters Δ and ν are correlated as Δ^2/ν in the motional narrowing region [see Eq. (14)], we deduced the hopping rate under the condition that Δ is a constant equal to its average determined in advance from the preliminary analysis.

In Fig. 12 the result is shown for the hopping rate deduced from the above analysis with $\Delta=0.390$ for sample A and $\Delta=0.386$ for sample B. From this result we can safely conclude that the difference of the hopping rate between samples A and B is totally negligible over the whole temperature region.

The temperature dependence of the hopping rate shows several distinct characteristics as obtained by the present measurement on both samples. In the following we describe currently accepted pictures of diffusion processes and compare them with the present experimental results.

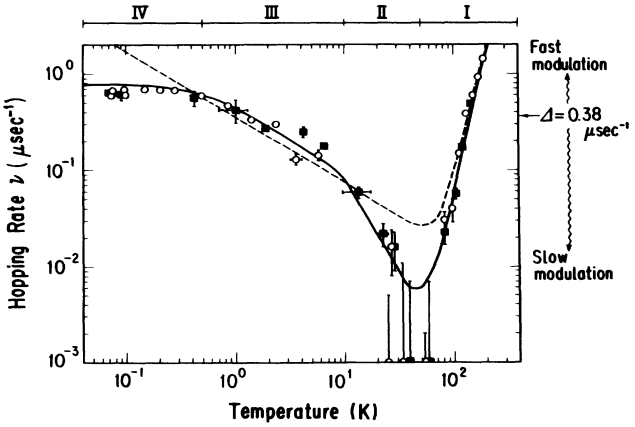

FIG. 12. Hopping rate of muon in pure copper. Open circle is A (RRR is 18 000); Andrew cross is copper B (RRR is 7350). The values were deduced under the fixed dipolar width. The solid and dashed curves show the theoretical calculations discussed in the text. The assigned parameter values are shown in Table III.

3. *Hopping rate: above ~100 K*

In the temperature region above $\sim10^2$ K, the hopping rate shows a temperature dependence of thermal activation type. As noted in the Introduction of this paper, this is well understood to be the phonon-assisted tunneling of a small polaron.[3–6] According to the theory of small-polaron diffusion,[3] the hopping rate is

$$\nu(T)=\nu_0\exp\left[-\frac{E_a}{kT}\right],$$
$$\nu_0=J_0^2\left[\frac{\pi}{4\hbar^2E_akT}\right]^{1/2}=\bar{\nu}_0\left[\frac{\Theta_D}{T}\right]^{1/2}, \tag{25}$$

where J_0 is the bare tunneling matrix of the small polaron, E_a is the activation energy so that the muon energy levels between the neighboring sites may coincide, k is the Boltzmann constant, and Θ_D is the Debye temperature (=343 K for copper). A more sophisticated form can be seen in Ref. 4. The analysis of our data at $100\sim190$ K by Eq. (25) gives

$$E_a/k=697\pm15\ \text{K}, \tag{26}$$

$$\bar{\nu}_0=(4.16\pm0.37)\times10^7\ \text{sec}^{-1}, \tag{27}$$

where $\bar{\nu}_0$ corresponds to $J_0^2(\pi/4\hbar^2E_ak\Theta_D)^{1/2}$. Consequently, we obtain the bare tunneling matrix J_0 as

$$J_0=36.1\pm3.2\ \mu\text{eV}. \tag{28}$$

These values are consistent with those reported in Ref. 2.

4. *Hopping rate: below ~10² K*

The hopping rate ν around $10\sim10^2$ K is fairly small compared with the dipolar width Δ. Since the hopping rate is determined mainly from the damping of the asymptotic tail of the relaxation function in this region [see Eq. (13)], the limit of the sensitivity of ν depends on the background B which determine the maximum time range reliable in the observed μ-e decay time spectrum. The typical value of B/N_0 in Eq. (4) is $10^{-5}\sim10^{-6}$, yielding a reliable time range of $25\sim30$ μsec. From this we can conclude that the hopping rate deduced by the analysis of the time spectrum at 0–15 μsec is free from background distortion.

Below about 50 K and down to 0.5 K the hopping rate increases with decreasing temperature. It was found from the present analysis with new data obtained by the improved measurement that the hopping rate has a steeper increase with decreasing temperature between $10\sim30$ K compared with that below 10 K.

The most distinctive feature of the hopping rate is seen in the temperature region below 10 K, where the behavior of ν is well described by a weak negative power of the temperature: $\nu\propto T^{-\alpha}$. A value $\alpha\sim0.4$ was deduced from the previous analysis.[24]

The present analysis with new data gives a larger value to the parameter α. The α depends on the temperature

region where the analysis is performed. The data between 0.5 and 10 K which seem to follow the above formula are well reproduced by

$$\nu \propto T^{-0.67\pm0.03}, \tag{29}$$

which coincides with the value ($\alpha=0.7$) estimated from the TF-μSR experiment.[12] In this case the data above 10 K show a small deviation from the curve extrapolated from the lower temperature. On the other hand, if we extend the temperature region of the analysis to the intermediate temperature 10–100 K, the parameter becomes $\alpha \simeq 0.80\pm0.02$.

It is only quite recently that the above hopping-rate behavior has got a sufficient explanation by the theories of Kondo[26,27] and Yamada.[28,29] According to their theories, the transition probability of a charged particle in metal is proportional to T^{2K-1}, where the factor T^{2K} comes from the nonadiabatic behavior of the conduction electrons following the motion of the particle. In other words, since the conduction electron can be excited by infinitely small energy (i.e., the infrared divergence), there is a kind of friction for charge-particle migration even via quantum-mechanical tunneling in metal.[52]

More specifically, following Kondo's assumption that the muon diffuses by hopping, the probability ν for the muon to jump to the neighboring sites is expressed as

$$\nu(T)=\frac{J^2}{\epsilon_F}\sqrt{\pi}\frac{\Gamma(K)}{\Gamma(\frac{1}{2}+K)}\left[\frac{\pi kT}{\epsilon_F}\right]^{2K-1}, \tag{30}$$

$$K=2V_0^2\rho^2\left[1-\frac{\sin^2 k_F a}{k_F^2 a^2}\right], \tag{31}$$

where $J(=J_0 e^{-S})$ is the tunneling matrix ($\hbar=1$) renormalized by phonon cloud, ϵ_F and k_F are the Fermi energy and momentum of conduction electrons, respectively, V_0 is the electronic potential produced by muon, ρ is the density of states per electronic spin, and a is the distance of migration by a single hop. $S=S(T)$ is determined by the muon-phonon interaction. The constant K is a measure of the strength of the muon-electron interaction. In the case of a singly charged particle K does not exceed $\frac{1}{2}$, so the exponent $2K-1$ is always negative.[53] The Eq. (30) is approximated for small K to give

$$\nu(T)=\frac{1}{kT\pi K}J^2\left[\frac{\pi kT}{\epsilon_F}\right]^{2K}=\rho_{\text{eff}}(J_{\text{eff}})^2 . \tag{32}$$

In the above expression the tunneling matrix element J is interpreted to be renormalized by $(\pi kT/\epsilon_F)^K$ due to the nonadiabaticity of the conduction-electron cloud, while another factor $\rho_{\text{eff}}=(\pi KkT)^{-1}$ comes from the broadening of the muon's energy level due to the interaction with the conduction electrons.

Even though obtaining the same temperature dependence for the muon transition probability, Yamada takes a different picture of coherent diffusion in which the factor $1/T$ is explained by the Korringa scattering by the conduction electrons. The difference will be discussed in the following section.

Using the α of Eq. (29), the constant K in Eq. (32) is

$$K=0.16\pm0.01 . \tag{33}$$

Although there is no prediction on the value of K, the above value is well below $\frac{1}{2}$ and consistent with the present interpretation.

As to the deviation of $\nu(T)$ from Eq. (32) at intermediate temperature (10^1–10^2 K), an effect due to the nonlinear coupling between muon and phonon was pointed out.[28,54] Historically, this coupling was first considered as an explanation of $\nu(T)$ below 10 K,[55] but the use of only this coupling is not sufficient to explain the observed weak-T dependence of $\nu(T)$ in copper.

Using the numerically calculated[54] hopping rate

$$\nu(T)=\frac{J_0^2}{\hbar k\Theta_D}H\left[\frac{T}{\Theta_D},S,K,d,\frac{\epsilon_F}{k\Theta_D}\right]$$

including all these mechanisms of diffusion up to 10^2 K, we analyzed the hopping-rate data above 0.5 K to examine the assumed theoretical models. Here parameter d is the coupling constant for the second-order muon-lattice interaction. The solid ($d\neq0$) and dashed ($d=0$) curves in Fig. 12 show the best-fit curves of $\nu(T)$, whose parameter values are summarized in Table III. The agreement between the experimental data and the solid curve in Fig. 12 is satisfactory, supporting such a nonlinear coupling described above.

Below 0.5 K the hopping rate shows a clear deviation from Eq. (29), which has already been reported in the earlier experiment.[10,23,24] In order to investigate the above behavior in detail, we performed an intensive set of measurements around this temperature region using the highest purity sample (A in Table I). As shown in Fig. 12, the observed $\nu(T)$ scarcely depends on temperature

TABLE III. Parameters deduced from the analysis of hopping rate by the theoretical function $\nu(T)=J_0^2/\hbar k\Theta_D H[T/\Theta_D,S,K,d,(\epsilon_F/k\Theta_D)]$. (See text for the definition of parameters.) Two different cases for $d=0$ and $d\neq0$ are shown (where d is the coupling constant to the nonlinear muon-lattice interaction). In both cases the parameter K was fixed to 0.16.

Parameters	$d=0$	$d\neq0$
$J_0^2/\hbar k$ (K μsec^{-1})	$(3.9\pm0.4)\times10^5$	$(1.6\pm0.3)\times10^6$
$\epsilon_F/\hbar\omega_D$	$(3.5\pm2.0)\times10^2$	200.0 (fixed)
S	5.69±0.05	6.58±0.06
Θ_D (K)	414.8±2.7	118.3±1.2
d		213.4±8.2

and has a plateau of $\nu(T)$ below 0.5 K. The hopping rate at the lowest temperature is independent of the residual resistivity ratio of samples (i.e., 7350 and 18 000).

5. *Level crossing resonance at 0.1 K*

It is well known that in copper around 20~80 K the muons predominantly occupy octahedral (O) interstitial sites.[7] To explain the leveling off of $\nu(T)$ below 0.5 K in pure copper, it has been held for a while that the muons might metastably occupy a tetrahedral (T) interstitial site at low temperatures.[13,56] Since the static dipolar width at the T site is estimated to be small compared with that of the O site, the change of relaxation function below 10 K could be interpreted as the increase of T-site occupation probability with decreasing temperature and its saturation below 0.5 K.

In order to directly investigate such a possible change of the localized state, we performed level-crossing resonance (LCR) measurements on sample A at 0.1 and 77 K. The time spectra were analyzed by the relaxation function $G_z(t)=e^{-\lambda t-\sigma t^2}$. The parameter λ was introduced to fit the motional narrowing. The results are shown in Fig. 13, where the Gaussian relaxation rate σ is plotted against the external magnetic field.

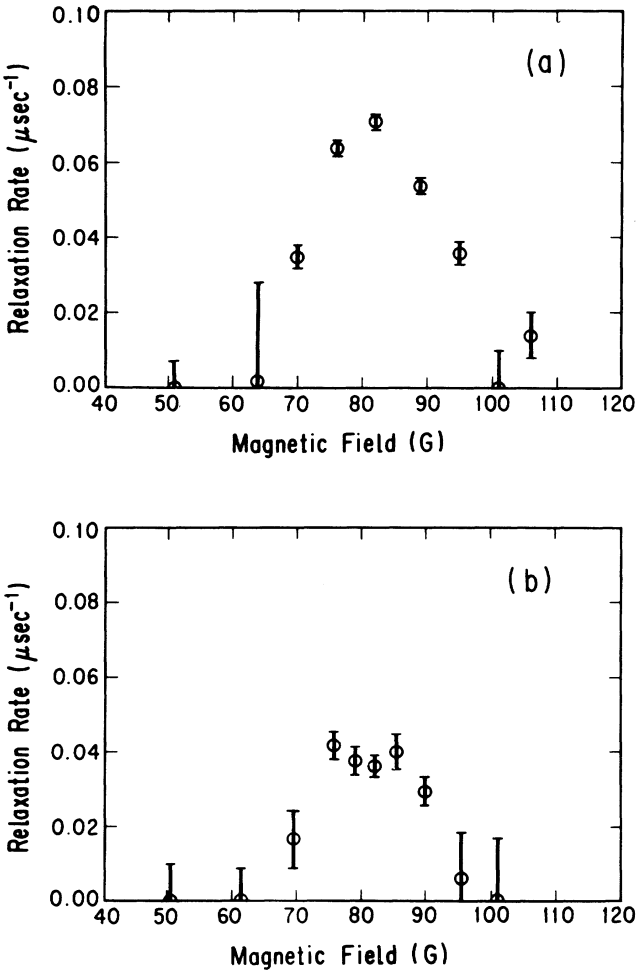

FIG. 13. Level-crossing resonance spectra of muon in pure copper at (a) 77 K and (b) 0.1 K. The Gaussian relaxation component σ is plotted against the external magnetic field.

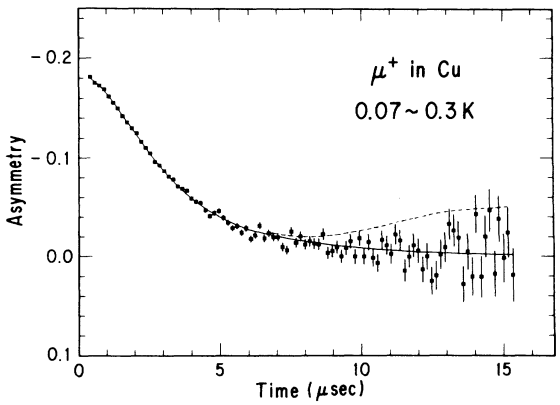

FIG. 14. The time spectrum summed over from 0.07 to 0.3 K. The solid curve indicates the best fit by Celio function with a fixed asymmetry determined at 4.2 K. No asymptotic recovery is seen up to 15 μsec. An example of the time spectrum predicted from the mixed site occupation is shown by a dashed curve.

As mentioned in Sec. II, the resonance spectrum at 77 K corresponds to a resolution function of LCR in copper (at O site) determined by the dipole-dipole interaction. Within resolution, it is hard to find a significant difference in the resonance field between 0.1 and 77 K. The reduction of resonance amplitude at 0.1 K is due to the motional narrowing which is absorbed in the parameter λ. The spectrum at 0.1 K suggests that there is some fine structure of resonance curve, which resembles the trend seen in Fig. 4(b). This result clearly indicates that a muon predominantly occupies O sites at 0.1 K during most of its lifetime.

There is another piece of experimental evidence which strongly supports the above conclusion. According to the simple assumption in Ref. 56, there are immobile muons initially localized at O sites, which should produce a residual asymptotic component in the ZF relaxation function at the "plateau" of the hopping rate. To examine this possibility, we summed the time spectra from 0.07 to 0.3 K to yield a high statistics spectrum below 0.5 K. As shown in Fig. 14 we could not find any trend to suggest such a recovery within our statistical accuracy (total events ~20 000 000).

B. Iron-doped copper

The aim of the measurement on the iron-doped copper was to see how the hopping rate is affected by an impurity. Several previous experiments with the same intent have been performed.[12,57] These show that the result is strongly dependent on the chemical nature of the impurities. We measured ZF-μSR spectrum on the 95-ppm iron-doped copper which was used in the TF-μSR measurement in Ref. 12.

In a preliminary analysis we found a sudden deviation of the relaxation function from the Celio function below 1 K. As shown in Fig. 15, below 1 K the minimum damping occurs earlier and is shallower than that of the Celio relaxation function.

Assuming that the residual moments of iron impurities produce additional local fields following an isotropic Lorentzian distribution

$$P^L(B)dB = \frac{\gamma_\mu^3}{\pi^2}\frac{a}{(a^2+\gamma_\mu^2 B^2)^2}4\pi B^2\,dB\ , \tag{34}$$

the static spin-relaxation function in this dilute spin glass is

$$g_z(t)=\tfrac{1}{3}+\tfrac{2}{3}(1-at-\Delta^2t^2)e^{-at-(\Delta^2t^2/2)}\ . \tag{35}$$

We have used the Kubo formula which connects $g_z(t)$ and $g_z(t)$, where the constant a/γ_μ corresponds to the root mean square of the residual local field from iron. In the above derivation, the nuclear dipolar field from copper was approximated by the Gaussian distribution [Eq. (6)]. The trend of the modification of the time spectra below 1 K are well explained by the above function with $a \simeq 0.2\Delta$.

The amplitude of a ($a/\gamma_\mu \sim 1$ G) is consistent with the value of the moment scaled from the value measured in the spin glass Cu(Mn) 1 at. % below the spin-glass transition temperature T_g [$a/\gamma_\mu \sim 10^2$ G at $T=0.5T_g$ (Ref. 58)]. This suggests the existence of an ordered phase (spin-glass-like) in such a dilute iron in copper. The above fact also implies that the muons are randomly distributed in the sample.

In any case, these results imply that the analysis by the Celio function is no longer valid below the glass-transition temperature. Although it may be possible to construct models to calculate the spin-relaxation function in a dilute spin glass, the analysis by such a relaxation function will be strongly model dependent.[58] In order to avoid such a model dependence, we utilized the fact that the asymptotic component of zero-field relaxation function is independent of the model of local magnetic field (aside from the difference between Kubo-Toyabe and Celio functions). Namely, after determining the asymmetry A from the analysis of the data above 1 K, we analyzed the later part (7.4 μsec $\sim$ 15 μsec) of spectrum below 1 K to deduce the damping rate of the asymptotic component.

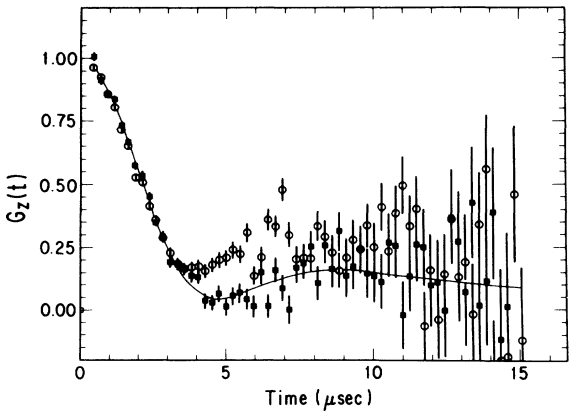

FIG. 15. The time spectrum of ZF-μSR in iron 95 at. % ppm doped Cu above and below 1 K. Solid square is data at 4.2 K; open circle is data at 0.6 K. Solid line indicates the best-fit curve of 4.2 K data by Celio function.

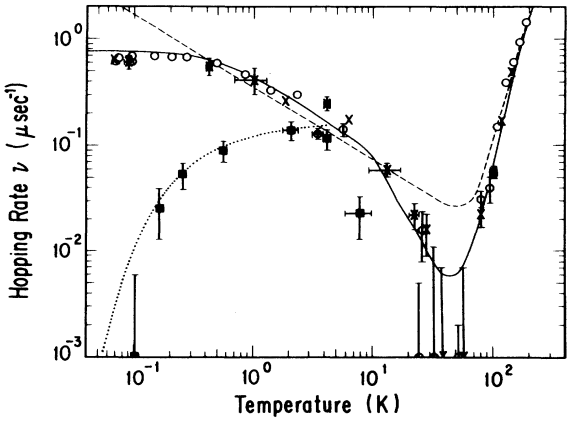

FIG. 16. Hopping rate of muon in iron-doped copper. The data are shown by solid squares. A fitting analysis for the data below 4.2 K gives $\nu_{Fe}(T) \propto \exp(-0.27\pm0.08\ K/T)$, which is shown as a dotted curve.

Taking into account that the local field on the muon is still dominated by the nuclear dipolar field, we used the asymptotic component of the Celio function for the fitting analysis. The deduced hopping rate is shown in Fig. 16 with the result in the previous section.

The result indicates that the hopping rate decreases again with decreasing temperature below 2 K, after showing an increase between 10 and 2 K. Because of the small value of the hopping rate, it is the present ZF-μSR experiment that first revealed such a temperature dependence. Despite the phase transition clearly seen in the dipolar width, there seems to be no steplike discontinuity in the hopping rate around 1 K. A preliminary result at higher temperature suggests that the difference of the hopping rate from that in pure copper is negligible above 4.2 K. The temperature dependence of the $\nu_{Fe}(T)$ resembles that of the thermally activated diffusion. We summarize the obtained experimental facts on iron doped copper.

(i) The temperature dependence of hopping rate is almost identical to the case of pure copper above 4 K. It should be emphasized that muon is *mobile* at around 4 K.

(ii) Muon is really *immobile* at 0.1 K which was confirmed by the observed full recovery of the asymptotic amplitude.

V. DISCUSSION

A. Hopping rate: below 10^1 K

1. *Muon-phonon interaction*

The μSR data in pure copper are interpreted in terms of a muon-electron interaction in combination with a nonlinear coupling to the phonons. With respect to the

phonons, two parameters are important: (i) the Debye temperature Θ_D and (ii) the nonlinear coupling strength d. As shown in Table III, concerning the Debye temperature we find a value of 118 K much lower than the copper value of $\Theta_D = 343$ K. On the other hand, without invoking the nonlinear coupling $\Theta_D = 414$ K considerably closer to 343 K is found, although the fit to the data is not as good as the previous case. We do not have a good explanation for this result other than that there must still be shortcomings in the theory as it concerns the phonon coupling. On the other hand, the value of S is consistent with the Debye approximation,

$$S(T=0)=\frac{5E_a}{2k\Theta_D} , \tag{36}$$

where if we insert $E_a = 697$ K from Eq. (26) and $\Theta_D = 343$ K we get $S = 5.08$ close to the value obtained from the fit. If one uses the full expression for small-polaron hopping[4] instead of the approximation used in Eq. (25), E_a would increase and the agreement would be even better.

2. *Muonic ground state in copper*

So far there is no other consistent theory to explain the temperature dependence of a hopping rate like Eq. (29) other than those by Kondo[26,27] and by Yamada.[28,29] Their independently developed theories describe the motion of charged particles interacting with conduction electrons in metals. As noted in the previous section, there is a fundamental difference between those two theories. Kondo assumes that the muonic ground state is localized while Yamada assumes it is a coherent Bloch wavelike state. To discuss which is closer to the reality it is interesting to examine the effective tunneling matrix element renormalized by the phonon cloud. As shown in Table III the effective tunneling matrix element $J = J_0 e^{-S}$ deduced from the analysis of $\nu(T)$ is about 1 μeV ($\sim 10^{-2}$ K) at low temperature. The mean free path l of a muon in a Bloch state is about[27]

$$\frac{l}{a_0} \sim \frac{J}{kT\pi g}\left[\frac{kT}{\epsilon_F}\right]^{2g} \quad \text{for } kT \gg J , \tag{37}$$

where a_0 is the lattice constant, and $g = 2V_0^2\rho^2$. Note that $g \geq K$ from Eq. (31). Since $kT \ll \epsilon_F$ is always satisfied in the present temperature range, the factor $(kT/\epsilon_F)^{2g}$ reduces the value of l/a_0 unless g is very small. For example, if we assume that $g \simeq K = 0.16$, the value of l/a_0 from Eq. (37) is roughly equal to 10^{-3} even at 0.1 K. From this we conclude that the mean free path of a muon is considerably smaller than the lattice constant over all the present temperature range. This small value of the mean free path seems to favor the picture of the localized muon in copper. The critical temperature T_C of the muonic ground state below which the Bloch state is the better approximation is deduced from the condition that $\nu(T) \sim J$ using Eq. (32) as

$$kT_C \sim J\left[\frac{J}{\epsilon_F}\right]^{K/1-K} , \tag{38}$$

T_C for copper is estimated to be 10^{-5} K.[54] Since the temperature region where the experiment is performed is always higher than T_C, we conclude that the migration of a muon should be ascribed to hopping motion in the measured temperature region. The localization of the muon wave function is also consistent with the insensitivity of the hopping rate to the difference of purity between samples A and B, on order of 1 ppm, which may be inferred from the difference in residual resistance ratio, 7350 and 18 000.

Experimentally, it might be possible to see whether such an extended muon state is realized or not. Namely, if Korringa scattering dominates the muon diffusion, an electronic current will affect (induce) the motion of muon along the current.[59]

3. *Effect of energy disorder on hopping rate*

We found that $\nu(T)$ shows a deviation (leveling off) from the theoretical function T^{2K-1} below 0.5 K. Kondo pointed out that such a deviation could be explained by some intrinsic disorder which causes a variation of the muonic energy level δ_E in a crystal.[27] Before we consider the origins of δ_E, we list the experimental results so far obtained by μSR in pure and iron-doped copper.

For the pure copper the following were obtained. (i) Both the LCR spectrum at 0.1 K and the time spectra for 0.07 ~ 0.3 K, with high statistical accuracy, give no evidence for a change of muon sites in copper below 0.5 K (present experiment). (ii) $\nu(T)$ is not affected by the improvement of the residual resistivity ratio of the copper sample (from 7350 to 18 000) (present experiment). (iii) The experiment is an isotope-enriched sample (99.88% ^{63}Cu) revealed that $\nu(T)$ is not affected by the difference of isotope mixture either.[12]

For the impurity doped copper we obtained the following results. (i) $\nu(T)$ is sensitive to the concentration of the impurity, i.e., 100 ppm iron causes large changes of $\nu(T)$ at low temperature (Ref. 12, present experiment). (ii) $\nu(T)$ is dependent on chemical difference of the doped impurities.[12,57] (iii) The estimated amplitude of a (i.e., the root mean square of the additional local field from iron moments) is consistent with the value expected from the spatial average of that arising from randomly oriented iron atomic moments (present experiment). (iv) Below 2 K the temperature dependence of $\nu(T)$ is quite similar to that for the thermal activation type (present experiment).

From result (i) for pure copper it is difficult to explain the observed leveling off of $\nu(T)$ as an effect of mixed-sites occupation among tetrahedral and octahedral interstitial sites. Meanwhile, a recent experiment of decay muon channeling from pion in copper showed that a significant fraction of pions decay at tetrahedral interstitial sites above 150 K and at octahedral sites below 150 K.[60] Nevertheless, it should be noted that the time range of measurement is different between muon and pion. The sensitive time range for the channeling experiment is determined by mean lifetime of pion (2.6×10^{-8} sec), while in our case it is determined by the static relaxation rate Δ ($\sim 10^{-6}$ sec). Therefore, if the lifetime of the meta-

stable state is close to that of pion, both results would be consistent with each other.

At the moment the most probable origin of the deviation of $\nu(T)$ from Eq. (30) below 0.5 K is the variation of muonic energy levels due to the defects and/or dislocations in a crystal arising from impurities, natural isotopes, and so on. If we assume that the crossover temperature T_δ of the $\nu(T)$ is roughly related to the energy fluctuation as $kT_\delta = \delta_E$, the present experiment suggests the magnitude of the δ_E as

$$\delta_E = \begin{cases} \sim 10^2\ \mu\text{eV for 100 ppm Fe in Cu}\ , \\ \sim 40\ \mu\text{eV for pure natural copper}\ . \end{cases} \tag{39}$$

According to the discussion in Ref. 12, the difference in energy levels Δ_E between two sites in copper separated by a distance d at the distance r away from a defect is

$$\Delta_E \simeq 1.04 \Delta^d \frac{d}{r^4}\ \text{eV}\ , \tag{40}$$

where Δ^d is the volume change produced by the defects. From the above formula they evaluate Δ_E at half-way between the impurities to be about 5 μeV for the 100-ppm iron impurity. Since a muon is randomly distributed in the copper, the spatial average of Eq. (40) ($=\langle \Delta_E \rangle$) should be considered in the case of dilute impurities to estimate the δ_E. The r dependence of Eq. (40) suggests that $\langle \Delta_E \rangle$ is much larger than 5 μeV. Although the formula does not apply for the natural isotope mixture of Cu^{63} and Cu^{65} because of the random overlap of strains, $\Delta_E \geq 100\ \mu$eV is shown from an extrapolation of the formula.[61] In any case these estimations for Δ_E (or $\langle \Delta_E \rangle$) show qualitative agreement with the experimental evaluation of δ_E.

The next problem is how we should understand the detailed behavior of $\nu(T)$ below 5 K in the pure and iron-doped samples. According to a phenomenological theory by Sugimoto,[62] the distribution of muonic energy levels should be taken into account for the evaluation of an effective hopping rate $\bar{\nu}(t)$ as

$$\bar{\nu}(T) = \int dE_i\, f(E_i) D(E_i) \int dE_f\, D(E_f) \int e^{-i(E_f - E_i)t} \phi(t) dt \Big/ \int f(E_i) D(E_i) dE_i \int D(E_f) dE_f\ , \tag{41}$$

where $\phi(t)$ is the transition (hopping) probability of a muon at a time t,[26,27] $f(E_i)$ is a probability function for the muon to occupy an initial energy E_i, $D(E)$ is the muonic energy level density, and E_f is the final-state muon energy. Hereafter we assume that the width of the distribution for the density function $D(E)$ is characterized by the energy $\delta_E = kT_\delta$.

There are several calculations using different assumptions on $f(E_i)$ and $D(E)$ in Ref. 62. The results indicate that the T dependence of $\nu(T)$ at low temperature strongly depend on the initial energy probability function $f(E_i)$. Namely, if we assume that $f(E_i)$ is a constant independent of energy, the consequent $\bar{\nu}(T)$ shows a plateau of the hopping rate below a characteristic temperature $T_\delta \simeq \delta_E/k$ irrespective of the shape of $D(E)$. The solid line in Fig. 12 (and Fig. 16) shows an example of $\bar{\nu}(T)$ calculated by using Eq. (41) and the following functions and parameters for $f(E_i)$ and $D(E)$:

$$D(E) = \begin{cases} 1/2\delta_E \text{ for } -\delta_E < E < \delta_E \\ 0 \text{ for } E < -\delta_E \text{ and } \delta_E < E \end{cases} \qquad \delta_E/k = 0.5\ \text{K}, \tag{42}$$

$$f(E_i) = 1\ .$$

On the other hand, if the function $f(E_i)$ takes a thermal equilibrium distribution like $e^{-\delta_E/kT}$ the calculated $\bar{\nu}(T)$ shows the temperature dependence approximated by

$$\bar{\nu}(T) \simeq J^2 \frac{\pi}{\delta_E} \left[\frac{kT}{\epsilon_F} \right]^{2K} \quad (kT \ll \delta_E)\ , \tag{43}$$

which decreases with decreasing temperature.[62] In this case we let a factor kT for the broadening of muonic final state due to the muon-electron interaction in Eq. (32) be replaced by $kT_\delta = \delta_E$ below T_δ.

The comparison between the above model and our experimental results in impurity-doped copper suggests that a thermal equilibrium distribution is favored for $f(E_i)$. Supposing that this is also the case for the pure copper, the plateau of $\nu(T)$ observed in the present experiment could be interpreted as a broad maximum of the hopping rate below which the hopping rate would begin to decrease with decreasing temperature. Otherwise, it might be an indication for the important role of impurity to the final step of muon thermalization process after the implantation.

B. Hopping rate: above 10^1 K

The present work makes it clear that the hopping rate is quite small in the range 10~100 K. Recently a new approach to determine the small hopping rate, i.e., the μSR measurement under low longitudinal field (LLF) was performed in copper at these intermediate temperatures.[41] The method has the advantage that the asymptotic component of the relaxation function is enhanced and thus one can measure a small damping rate with better statistical accuracy. However, it was found that the hopping rate determined by the LLF method was systematically larger (by about 0.03 μsec^{-1}) than our data by ZF method. It is important to determine the origin(s) of this discrepancy.

The sensitivity range for measuring a small hopping rate is determined by the condition that the modulation of the relaxation function is comparable to the amplitude of the statistical or systematic errors in a realistic experiment. In the present experiment the main source of systematic error is thought to be the counting loss of positrons, which would cause a distortion of spectrum typi-

cally around 0.7% [i.e., 4% of $G_z(t)$] near $t=0$. This is comparable to a change of the ZF relaxation function at $t=15$ μsec by the change of the modulation frequency from $\nu=0$ to $\nu\simeq 0.01$ μsec^{-1}. Supposing that the distortion propagates to the later part (tail) of the time spectrum through the fitting procedures, we roughly estimate that the sensitivity limit of the hopping rate is around $\nu=0.01$ μsec^{-1}. Since the correction for the counting loss is possible, the practical sensitivity limit for ν should be smaller than the above value. From this discussion we conclude that our observed temperature dependence of the hopping rate between $10^1\sim 10^2$ K is valid, unless ν is far below 0.01 μsec^{-1}.

It should be noted that the statistical accuracy is rather indifferent to the systematic errors. There are at least two possible explanations related to the systematic errors for the disagreement of hopping rate between our result and that in Ref. 41.

First, the limit of the observable range of the correlation time is determined by the width of the time window of the measurement, which is chiefly determined by the background level. As noted in Sec. III A we have advantages at least on this point. Namely, in our case the background was about 10^{-5} for all the measured ZF-μSR time spectra, making it possible to reliably measure up to 20 μsec. While the background for a dc beam as in Ref. 41 is usually of order of 10^{-3} or greater, although they make no reference to it.

The other source of possible systematic error in the LLF method is found in the process to determine the experimental asymmetry A. According to Ref. 41, the initial ($t=0$) amplitude of the positron decay asymmetry was determined by the TF spin-rotation amplitude in a separate experiment. In this case, supposing that there were a small fraction of muons which stopped in the surrounding materials (e.g., cryogenic vessels, muon-defining counters, etc.), this fraction can also contribute to the precession amplitude. While in the LLF condition, the positron signal from such a fraction contributes only as a time-independent bias in the time spectrum. This means that the initial asymmetry determined from TF-μSR is possibly different from the true value in LLF condition. ZF measurements are rather free from such an ambiguity, where the asymmetry is determined by the time spectrum in a self-consistent manner.

C. Conclusions

In this paper we have reported on an experimental investigation of muon diffusion in copper of different purities. Following, we summarize the present work.

(1) Using zero-field μ-SR the hopping rate of muon in copper was directly observed in a wide temperature range of $10^{-1}\sim 10^{2.5}$ K.

(2) In pure copper the hopping rate has a distinctive temperature dependence $\nu(T)\propto T^{-\alpha}$ with $\alpha=0.67\pm 0.03$ between 0.5 and 10 K.

(3) The observed $\nu(T)$ at $10\sim 30$ K has a steeper temperature dependence than the lower temperature region, which we explain as arising from a nonlinear coupling between phonon and muon.

(4) There is a plateau of $\nu(T)$ below 0.5 K, which so far remains a puzzle. The experiment showed that the plateau is not due to impurities, nor to a spurious result from a changed preferential site of a muon in the crystal. The crossover temperature ($=0.5$ K) is consistent with a rough estimation of the energy disorder due to the isotope mixture of ^{63}Cu and ^{65}Cu in natural copper.

(5) The temperature dependence of the hopping rate is sensitive to the impurities of order of 100 ppm in the experiment on iron-doped copper.

As a future possibility, the present study should be extended to the much lower temperature down to 10^{-3} K or more to determine whether the plateau of $\nu(T)$ extends or not, especially in pure copper. This would be useful for the understanding of this plateau.

ACKNOWLEDGMENTS

We would like to thank all the members of Meson Science Laboratory, especially Dr. Y. Kuno (TRIUMF) for his support of our experiment. Thanks are also due to the long-time collaborators in TRIUMF, especially to Professor J. H. Brewer for his continuous help and interest, and also to Dr. M. Celio for his help using his new relaxation function. We acknowledge Professor J. Kondo, Professor K. Yamada, and Professor R. Kubo for their theoretical support and stimulating discussions on our experimental investigation. We also acknowledge helpful discussion with Dr. H. Sugimoto. This work is partially supported by the Grant-in-Aid of the Ministry of Education, Science and Culture.

*Present address: TRIUMF, 4004 Wesbrook Mall, Vancouver, B.C., Canada V6T2A3.

†Present address: National Laboratory for High Energy Physics, Oho-machi, Tsukuba-gun, Ibaraqi-ken 305, Japan.

‡Present address: The Institute of Physical and Chemical Research, Wako-shi, Saitama-ken 351-01, Japan.

§Present address: Institute for Nuclear Study, University of Tokyo, 3-2-1 Midori-cho, Tanashi-shi, Tokyo 188, Japan.

**Present address: Institut Laue-Langevin, 156X, 38042 Grenoble Cedex, France.

[1]I. I. Gurevich, E. A. Mel'eshko, I. A. Muratova, B. A. Nikol'sky, V. S. Roganov, V. I. Selivanov, and B. V. Sokolov, Phys. Lett. **40A**, 143 (1972).

[2]V. G. Grebinnik, I. I. Gurevich, V. A. Zhukov, A. P. Manich, E. A. Mel'eshko, I. A. Muratova, B. A. Nikol'sky, V. I. Selivanov, and V. A. Suetin, Zh. Eksp. Teor. Fiz. **68**, 1548 (1975) [Sov. Phys.—JETP **41**, 777 (1975)].

[3]C. P. Flynn and A. M. Stoneham, Phys. Rev. B **1**, 3966 (1970).

[4]H. Teichler, Phys. Lett. **64A**, 78 (1977).

[5]H. Teichler, Phys. Lett. **67A**, 313 (1978); Hyp. Int. **6**, 251 (1979).

[6]D. Emin, Hyp. Int. **8**, 515 (1981).

[7]M. Camani, F. N. Gygax, W. Rüegg, A. Schenck, and H. Schilling, Phys. Rev. Lett. **39**, 836 (1977).

[8]O. Hartmann, Phys. Rev. Lett. **39**, 832 (1977).

[9]J. H. Van Vleck, Phys. Rev. **74**, 1168 (1948).

[10]O. Hartmann, E. Karlsson, L. O. Norlin, T. O. Niinikoski, K. W. Kehr, D. Richter, J.-M. Welter, A. Yaouanc, and J. Le Hericy, Phys. Rev. Lett. **44**, 337 (1980).
[11]O. Hartmann, L. O. Norlin, A. Yaouanc, J. Le Hericy, E. Karlsson, and T. O. Niinikoski, Hyp. Int. **8**, 533 (1981).
[12]J.-M. Welter, D. Richter, R. Hempelmann, O. Hartmann, E. Karlsson, L. O. Norlin, T. O. Niinikoski, and D. Lenz, Z. Phys. B **52**, 303 (1983).
[13]A. Seeger, Phys. Lett. **93A**, 33 (1982).
[14]R. S. Hayano, Y. J. Uemura, J. Imazato, N. Nishida, T. Yamazaki, H. Yasuoka, and Y. Ishikawa, Phys. Rev. Lett. **41**, 1743 (1978).
[15]Y. J. Uemura, R. S. Hayano, J. Imazato, N. Nishida, and T. Yamazaki, Solid State Commun. **31**, 731 (1979).
[16]R. S. Hayano, Y. J. Uemura, J. Imazato, N. Nishida, T. Yamazaki, and R. Kubo, Phys. Rev. B **20**, 850 (1979).
[17]T. Yamazaki, Hyp. Int. **6**, 115 (1979).
[18]R. Kubo and T. Toyabe, in *Magnetic Resonance and Relaxation,* edited by R. Blinc (North-Holland, Amsterdam, 1967).
[19]K. G. Petzinger, Phys. Lett. **75A**, 225 (1980); Hyp. Int. **8**, 639 (1981).
[20]C. Boekema, R. H. Heffner, R. L. Hutson, M. Leon, M. E. Schillaci, W. J. Kossler, M. Numan, and S. A. Dodds, Phys. Rev. B **26**, 2341 (1982).
[21]C. W. Clawson, K. M. Crowe, S. E. Kohn, S. S. Rosenblum, C. Y. Huang, J. L. Smith, and J. H. Brewer, Physica **109&110B**, 2164 (1982).
[22]C. W. Clawson, K. M. Crowe, S. S. Rosenblum, S. E. Kohn, C. Y. Huang, J. L. Smith, and J. H. Brewer, Phys. Rev. Lett. **51**, 114 (1983).
[23]R. Kadono, J. Imazato, K. Nishiyama, K. Nagamine, T. Yamazaki, D. Richter, and J.-M. Welter, Hyp. Int. **17-19**, 109 (1984).
[24]R. Kadono, J. Imazato, K. Nishiyama, K. Nagamine, T. Yamazaki, D. Richter, and J.-M. Welter, Phys. Lett. **109A**, 61 (1985).
[25]R. Kadono, T. Matsuzaki, K. Nagamine, T. Yamazaki, D. Richter, and J.-M. Welter, Hyp. Int. **31**, 205 (1986).
[26]J. Kondo, Physica **125B**, 279 (1984).
[27]J. Kondo, Physica **126B**, 377 (1984).
[28]K. Yamada, Prog. Theor. Phys. **72**, 195 (1984).
[29]K. Yamada, A. Sakurai, and S. Miyazawa, Prog. Theor. Phys. **73**, 1342 (1985).
[30]A. Schenck, *Muon Spin Rotation Spectroscopy* (Adam Hilger, Bristol, 1985).
[31]A. Abragam, C. R. Acad. Sci. Ser. 2 **299**, 95 (1984).
[32]S. R. Kreitzman, J. H. Brewer, D. R. Harshman, R. Keitel, D. Ll. Williams, K. M. Crowe, and E. J. Ansaldo, Phys. Rev. Lett. **56**, 181 (1986).
[33]M. Celio and P. F. Meier, Phys. Rev. B **27**, 1908 (1983); Hyp. Int. **17-19**, 435 (1984).
[34]K. G. Petzinger and S. H. Wei, Hyp. Int. **17-19**, 441 (1983).
[35]R. Kadono, J. Imazato, K. Nishiyama, K. Nagamine, T. Yamazaki, D. Richter, and J.-M. Welter, Phys. Lett. **107A**, 279 (1985).
[36]E. Holzschuh and P. F. Meier, Phys. Rev. B **29**, 1129 (1984).
[37]M. Celio, Phys. Rev. Lett. **56**, 2720 (1986); Hyp. Int. **31**, 41 (1986).
[38]R. Kubo, J. Phys. Soc. Jpn. **9**, 935 (1954).
[39]R. Kubo, Hyp. Int. **8**, 731 (1981).
[40]K. W. Kehr, G. Honig, and D. Richter, Z. Phys. B **32**, 49 (1978).
[41]J. H. Brewer, M. Celio, D. R. Harshman, R. Keitel, S. R. Kreitzman, G. M. Luke, D. R. Noakes, R. E. Turner, E. J. Ansaldo, C. W. Clawson, K. M. Crowe, and C. Y. Huang, Hyp. Int. **31**, 191 (1986).
[42]R. Kubo (private communication).
[43]R. Kubo and K. Tomita, J. Phys. Soc. Jpn. **9**, 888 (1954).
[44]S. R. Kreitzman, Hyp. Int. **31**, 13 (1986).
[45]K. Nagamine, Hyp. Int. **8**, 787 (1981).
[46]K. W. Kehr, D. Richter, J.-M. Welter, O. Hartmann, E. Karlsson, L. O. Norlin, T. O. Niinikoski, and A. Yaouanc, Phys. Rev. B **26**, 567 (1982).
[47]O. V. Lounasmaa, *Experimental Principles and Methods Below 1K* (Academic, London, 1974).
[48]Y. Kuno, K. Nishiyama, R. S. Hayano, J. Imazato, H. Nakayama, K. Nagamine, and T. Yamazaki, Proceedings of the 1981 INS International Symposium on Nuclear Radiation Detectors, 1981, Tokyo, Japan (unpublished).
[49]T. Yamazaki, R. S. Hayano, Y. Kuno, S. Ohtake, and T. Nagae, Nucl. Instrum. Methods **196**, 289 (1982); Y. Kawashima, Y. Watanabe, and T. Yamazaki, Hyp. Int. **32**, 873 (1986).
[50]W. T. Eadie, D. Dryard, F. E. James, M. Roos, and B. Sadoulet, *Statistical Methods in Experimental Physics* (North-Holland, Amsterdam, 1971).
[51]F. James and M. Roods, MINUIT—A System for Function Minimization and Analysis of the Parameter Errors and Correlations, CERN Computer 7600 Interim Programme Library (1971) (unpublished).
[52]U. Weiss and H. Grabert, Phys. Lett. **108A**, 63 (1985).
[53]K. Yamada and K. Yosida, Prog. Theor. Phys. **68**, 1504 (1982).
[54]J. Kondo, Hyp. Int. **31**, 117 (1986).
[55]Y. Kagan and M. I. Klinger, J. Phys. C **7**, 2791 (1974).
[56]A. Seeger and L. Schimmele, Hyp. Int. **17-19**, 133 (1984).
[57]J. Chappert, A. Yaouanc, O. Hartmann, E. Karlsson, L.-O. Norlin, and T. O. Niinikoski, Solid State Commun. **44**, 13 (1982).
[58]Y. J. Uemura, UT-MSL Report No. 20 (Ph.D. thesis, University of Tokyo, 1982).
[59]K. M. Crowe and A. M. Portis, Hyp. Int. **31**, 185 (1986).
[60]G. Flik, J. Bradbury, W. Cooke, M. Leon, M. Paciotti, M. Schillaci, K. Maier, H. Rempp, and A. Seeger, Hyp. Int. **31**, 61 (1986).
[61]See also, A. M. Stoneham, in *Exotic Atoms 1979,* edited by K. Crowe, J. Duclos, G. Fiorentini, and G. Torelli (Plenum, New York, 1980), p. 223.
[62]H. Sugimoto, J. Phys. Soc. Jpn. **55**, 1687 (1986).